ABSTRACT

Title of dissertation: ORBITAL-FREE
DENSITY FUNCTIONAL THEORY
OF ATOMS, MOLECULES, AND SOLIDS

Jeng-Da Chai, Doctor of Philosophy, 2005

Dissertation directed by: Professor John D. Weeks
Institute for Physical Science and Technology
Department of Chemistry and Biochemistry

Density functional (DF) theory has proved to be a powerful way to determine the ground state energy of atoms, molecules, and extended systems. An important part of the theory requires one to determine the kinetic energy of the ground state of a system of N noninteracting electrons in a general external field. Kohn and Sham showed how this can be numerically calculated very accurately using a set of N orbitals. However this prevents the simple linear scaling in N that would arise if the kinetic energy could be directly expressed as a functional of the electron density, as is done with other components of the total energy like the exchange-correlation energy. Orbital free methods attempt to calculate the noninteracting kinetic energy directly by approximating the universal but unknown kinetic energy density functional. However simple local approximations are inaccurate and it has proved very difficult to devise generally accurate nonlocal approximations. We focus instead on the kinetic potential, the functional derivative of the kinetic energy DF, which appears in the Euler equation for the electron density. We argue the kinetic

potential is more amenable to simple physically motivated approximations in many relevant cases. We propose a family of nonlocal orbital free kinetic potentials that reduce to the known exact forms for both slowly varying and rapidly varying perturbations and also reproduce exact results for the linear response of the density of the homogeneous system to small perturbations. A simple and systematic approach for generating accurate and weak *ab initio* local pseudopotentials describing a smooth slowly varying valence component of the electron density is proposed for use in orbital free DF calculations of molecules and solids. The use of these local pseudopotentials further minimizes the possible errors arising from use of the approximate kinetic potentials. A linear scaling method for treating large extended systems is proposed for fast computations. Our theory yields results for the total energies and ionization energies of atoms, and for the shell structure in the atomic radial density profiles that are in very good agreement with calculations using the full Kohn-Sham theory. We describe the first use of nonlocal orbital free methods to determine the ground-state bond lengths and binding energies of diatomic molecules. These results and the ground-state lattice parameters, and total energy of bulk aluminum and bulk silicon are in generally good agreement with detailed calculations using the full Kohn-Sham theory.

ORBITAL-FREE DENSITY FUNCTIONAL THEORY OF ATOMS, MOLECULES, AND SOLIDS

by

Jeng-Da Chai

Dissertation submitted to the Faculty of the Graduate School of the
University of Maryland, College Park in partial fulfillment
of the requirements for the degree of
Doctor of Philosophy
2005

Advisory Commmittee:

Professor John D. Weeks, Chair/Advisor
Professor Millard H. Alexander
Professor Theodore R. Kirkpatrick
Professor Daniel S. Kosov
Professor Victor M. Yakovenko

DEDICATION

To my parents, my brother, Lan, Man-Chiao, and Ivy

ACKNOWLEDGMENTS

First, I would like to thank my Ph.D. thesis advisor, Prof. John D. Weeks, for his guidance, giving me this opportunity and allowing me the independence in designing the theoretical framework developed in this work. I would also like to thank him for being very flexible and understanding during some tough personal situations that I faced.

I would like to thank my M.S. thesis advisor, Prof. David G. Stroud at the Ohio State University, for his advice and encouragement on my past research.

I want to thank Prof. Emily A. Carter at Princeton University, for her hospitality during my visit to Princeton University, where the work on solids discussed in Chapter 5 of this thesis was begun. Without this collaboration and the use of her computer programs and computer facilities, this work could not have been completed. I am also grateful for the help and scientific conversations provided by her group members, Gregory Ho and Vincent Ligneres.

Thanks are due to my committee, Prof. Millard H. Alexander, Prof. Theodore R. Kirpatrick, Prof. Daniel S. Kosov, and Prof. Victor M. Yakovenko, for their participation and their useful comments on this dissertation.

I am grateful to Prof. J. Robert Dorfman, for his serving as the substitute chair of my dissertation committee.

I want to thank Prof. Michael E. Fisher, for his useful comments on this work.

I want to thank my past and present group members, Dr. Tong Zhao, Dr. Yng-gwei Chen, Dr. Charanbir Kaur, Dr. Madhav Ranganathan, and Jocelyn Rodgers, for their friendship and scientific conversations.

I am especially grateful to Lan, Man-Chiao, and Ivy, for their warm support and friendship through different phases of my graduate study.

Most of all, I want to thank my parents and brother for their love and encouragement.

TABLE OF CONTENTS

LIST OF TABLES

LIST OF FIGURES

Chapter 1

Introduction

1.1 Overview

Modern quantum theories based on determining electronic orbitals and wavefunctions have led to significant progress in understanding the electronic structure of atoms, molecules, and solids. In traditional approaches, in order to calculate the ground state energy and electron density for a system with N electrons, one uses the Schrödinger equation and tries to determine the ground state wavefunction $\Psi(r_1, s_1, \cdots, r_N, s_N)$, a complicated function of the space and spin coordinates for each electron. The Hartree-Fock (HF) method considers a simplified wavefunction made up of a properly symmetrized product of single electron orbitals. This can be quite useful in some cases and it serves as the starting point for more accurate methods like configuration interaction (CI) and coupled cluster approaches (CC), which account for the correlation energy neglected in the HF method. However there are important phenomena involving many electrons and occurring on large length scales, where the traditional orbital-based quantum mechanical approaches are intractable. For example, the formal scaling of the HF method with the number of electrons is $O(N^4)$. Methods treating electron correlations have even worse scaling. For example, the formal scaling of CCSD(T) (couple cluster method with single and double excitations, and perturbative treatment in the triple excitation) is

$O(N^7)$. This expensive scaling prevents a general study of large quantum systems except in special high symmetry cases.

As a result, it is important to develop approximate quantum mechanical methods to qualitatively account for quantum effects in such large systems. One of the most appealing candidates is orbital-free density functional theory (OF-DFT). Here the electron density $\rho(\mathbf{r})$, a function of only three variables, is the only physically significant quantity needed in the theory. The computational cost of such an approach can be dramatically reduced for large systems when compared with traditional methods. This dissertation provides both a new physical understanding and theoretical development of OF-DFT. Our theory represents the first unified and reasonable accurate application of the same OF method to a wide variety of quantum systems, ranging from atoms to molecules and solids. The results of the present OF-DFT are compared to those of earlier OF-DFT's, to the accurate Kohn-Sham DFT (discussed below), and to experiment.

1.2 Density Functional Theory and the Kohn-Sham Method

Density-functional theory (DFT) has become one of the most powerful tools for investigating the electronic structure of large systems (up to several hundreds of particles), which the traditional quantum chemistry methods, such as Hartree-Fock (HF) and configuration interaction (CI) methods, can hardly handle because of their expensive scaling with system size [1, 2]. As shown by Hohenberg and Kohn (HK) [3], the exact ground state energy of a system of N electrons can be formally

written as a functional $E[\rho]$ of the electron density $\rho(\mathbf{r})$ and the external field $V_{ext}(\mathbf{r})$ only. Kohn and Sham (KS) [4, 5] showed $E[\rho]$ can be usefully partitioned into the following set of terms:

$$E[\rho] = T_s[\rho] + E_H[\rho] + E_{xc}[\rho] + \int \rho(\mathbf{r}) V_{ext}(\mathbf{r}) d\mathbf{r}. \tag{1.1}$$

Here $T_s[\rho]$ is the *noninteracting kinetic energy density functional* (KEDF), which gives the kinetic energy of a model system of N noninteracting electrons in a self-consistent field chosen so that the ground state density equals $\rho(\mathbf{r})$,

$$E_H[\rho] \equiv \frac{1}{2} \int \int \frac{\rho(\mathbf{r})\rho(\mathbf{r}')}{|\mathbf{r} - \mathbf{r}'|} d\mathbf{r} d\mathbf{r}' \tag{1.2}$$

is the classical *electron-electron potential energy* (Hartree energy) and $E_{xc}[\rho]$ is the *exchange-correlation energy* (including the difference between the interacting and noninteracting kinetic energy and the difference between the quantum and classical electron-electron potential energy). The last term on the right of Eq. (1.1) is the only term that depends explicitly on the external potential $V_{ext}(\mathbf{r})$. Atomic units are used throughout the dissertation, unless noted otherwise.

If these functionals were all known, then the density $\rho(\mathbf{r})$ could be obtained from the variational principle (Euler equation) associated with minimizing Eq. (1.1):

$$\mu = V_{T_s}(\mathbf{r}; [\rho]) + V_{eff}(\mathbf{r}; [\rho]), \tag{1.3}$$

and the total energy of the inhomogeneous system could then be determined from the energy functional $E[\rho]$. All other physical quantities related to the ground-state density could also be computed. Here μ is the chemical potential (the Lagrange multiplier associated with the normalization condition $\int \rho(\mathbf{r}) d\mathbf{r} = N$), and $V_{eff}(\mathbf{r}; [\rho])$

is an effective one-body potential with the form

$$\begin{aligned} V_{eff}(\mathbf{r};[\rho]) &\equiv \frac{\delta}{\delta\rho(\mathbf{r})}\{E_H[\rho] + E_{xc}[\rho] + \int \rho(\mathbf{r})V_{ext}(\mathbf{r})d\mathbf{r}\} \\ &= V_H(\mathbf{r};[\rho]) + V_{xc}(\mathbf{r};[\rho]) + V_{ext}(\mathbf{r}), \end{aligned} \tag{1.4}$$

where

$$V_H(\mathbf{r};[\rho]) \equiv \delta E_H[\rho]/\delta\rho(\mathbf{r}) = \int \frac{\rho(\mathbf{r}')}{|\mathbf{r}-\mathbf{r}'|}d\mathbf{r}' \tag{1.5}$$

is the *Hartree potential*, and $V_{xc}(\mathbf{r};[\rho]) \equiv \delta E_{xc}[\rho]/\delta\rho(\mathbf{r})$ is the *exchange-correlation potential*. Similarly we interpret

$$V_{T_s}(\mathbf{r};[\rho]) \equiv \delta T_s[\rho]/\delta\rho(\mathbf{r}) \tag{1.6}$$

as the *kinetic potential* (KP) arising from the KEDF [6].

Although the exact forms of $T_s[\rho]$ and $E_{xc}[\rho]$ are not known, KS showed that the numerical value of the noninteracting kinetic energy can be exactly determined, not directly from the density itself using $T_s[\rho]$, but by introducing a set of N one-electron wave functions (orbitals) satisfying the N coupled equations that describe the model system [4, 5]. Their approach is as follows. Eq. (1.3) with the normalization condition is exactly the same equation as one obtains from DFT, when one applies it to a *noninteracting* system, where electrons are moving in the external potential $V_{eff}(\mathbf{r})$ in Eq. (1.4). For such a reference system, one can simply solve N one-electron equations [1]

$$[-\frac{1}{2}\nabla^2 + V_{eff}(\mathbf{r})]\psi_i(\mathbf{r}) = \epsilon_i\psi_i(\mathbf{r}) \tag{1.7}$$

where ϵ_i are the orbital energies, and the orbitals $\psi_i(\mathbf{r})$ are chosen to be orthonormal.

The electron density is then

$$\rho(\mathbf{r}) = \sum_i \mid \psi_i(\mathbf{r}) \mid^2 \tag{1.8}$$

Equations (1.4,1.7,1.8) are the KS equations and have to be solved self-consistently. One starts with a trial density, constructs $V_{eff}(\mathbf{r})$ from Eq. (1.4), and then obtains a new density from Eq. (1.7) and Eq. (1.8). This process is repeated, until the constructed $V_{eff}(\mathbf{r})$ exactly reproduces the density that generates the same $V_{eff}(\mathbf{r})$. After obtaining the ground-state electron density and orbitals, the numerical value of the kinetic energy $T_s[\rho]$ can then be computed as

$$T_s[\rho] = \sum_i \int \psi_i(\mathbf{r})(-\frac{\nabla^2}{2})\psi_i(\mathbf{r})d\mathbf{r} \tag{1.9}$$

Through the efforts of many workers we now have rather accurate expressions for $E_{xc}[\rho]$, whose magnitude is generally much smaller than that of the kinetic energy. Thus using these orbitals one can accurately determine both the total energy $E[\rho]$ and the ground-state density $\rho(\mathbf{r})$ of a wide variety of systems with currently available $E_{xc}[\rho]$.

This accurate treatment of the kinetic energy played a central role in the development of DFT as a quantitative method [1]. The KS method has yielded very accurate ground-state densities and energies for many systems. In many cases even a simple local density approximation for $E_{xc}[\rho]$ proves adequate, and we will use this in most of results reported here. Moreover, the accuracy of KS-DFT led to the development of *ab initio* molecular dynamics (AIMD) methods, where the forces on the nuclei as the nuclei move are determined using KS-DFT [7], while the nuclear motion is treated classically. KS-AIMD has become one of the most powerful and

widely used tools for studying the dynamics of a wide variety of chemical processes in both the liquid and solid states [8, 9, 10, 11].

However, the numerical cost of self-consistently determining N orbitals normally scales as $O(N^3)$. While this is a much better scaling than traditional quantum chemistry methods treating electron correlation, it still is prohibitive for large systems. In recent years, there have been some theoretical developments that can reduce the cubic scaling in KS-DFT in some cases, using the so-called orbital-based linear scaling techniques [12], which are based on the "locality" of different pieces of a large quantum system. However, a very large prefactor still remains in these methods, and they become cheaper than the conventional KS-DFT only for very large numbers of atoms (larger than 100 atoms). Furthermore, the assumption of locality prevents these approaches from studying metallic systems, where the orbitals cannot be exponentially localized. As a result, simulations of the evolution of larger systems (more than a few thousands of particles) over longer times (several tens of ps) are still not possible. An accurate treatment of the kinetic energy as well as the potential energy contributions in terms of the electron density only, as originally envisioned in the work of HK, would certainly be desirable.

1.3 Orbital-Free DFT and the Thomas-Fermi Model

Due to the expensive scaling of the KS orbital methods, an accurate treatment of the kinetic energy as well as the potential energy contributions in terms of the electron density only could have a major impact in practical calculations [1, 2, 13].

To that end there has been considerable effort invested in developing "orbital-free density functional theory" (OF-DFT) by making direct approximations for $T_s[\rho]$ [14, 15, 16, 17, 18, 19, 20, 21, 22, 23, 24, 25, 26, 27]. Due to its fast computation and qualitative description of quantum systems, OF-DFT has also been combined with AIMD, and has led to the so-called OF-AIMD. Recently, OF-AIMD has been successfully applied to study the static and dynamic property of some extended systems with thousands of atoms [28, 29, 30].

The first direct approximation for $T_s[\rho]$ is the Thomas-Fermi (TF) model [31], which is exact for a uniform system:

$$T_{TF}[\rho] = C_F \int \rho^{5/3}(\mathbf{r}) d\mathbf{r}, \tag{1.10}$$

where $C_F = \frac{3}{10}(3\pi^2)^{2/3}$. The TF model is derived by local use of a uniform free electron gas model and is known to be exact in the limit of an infinite number of electrons [32]. However, for an atomic system, the number of electrons N is finite, the electron density is far from constant, and the effective potential is very rapidly varying near the nucleus. As a result, there are many deficiencies in the TF model for such applications. The total energies predicted for atomic systems give at best an order of magnitude estimate, and cannot be relied on for quantitative calculations. More serious errors can be seen in the density response at particular values of $\mathbf{r}$ as determined from the Euler equation (1.3). For example, the TF model predicts an infinite electron density at the nucleus. In addition, the density does not decay exponentially in the classically forbidden region (the tail region), and it does not show any shell structure. Furthermore, the TF model predicts no atomic bonding

to form molecules or solids [33, 34]. Though the TF model has many shortcomings, it is a natural local approximation and gives a simple analytical expression for the KEDF and the KP.

By considering modified plane waves of the form $(1+\mathbf{a}\cdot\mathbf{r})e^{i\mathbf{k}\cdot\mathbf{r}}$, with $\mathbf{a}$ a constant vector and $\mathbf{k}$ the local wave vector, von Weizsäcker [35] derived a correction

$$T_W[\rho] = \frac{1}{8}\int \frac{|\nabla\rho(\mathbf{r})|^2}{\rho(\mathbf{r})}d\mathbf{r} \tag{1.11}$$

to the TF kinetic energy functional:

$$T_{TFW}[\rho] = T_{TF}[\rho] + T_W[\rho]. \tag{1.12}$$

Its self-consistent use in Eq. (1.3) for atoms not only yields a finite electron density at the nucleus, but also gives the correct exponential decay of the density far from the nucleus [36, 37] for the exact μ. We refer to this as the TFW model. Disappointingly, however, the kinetic energy given by this approach is not much better than that of the original TF model.

Based on the TFW model, the main advance in recent work has been to introduce *nonlocal* KEDFs that reproduce the known exact results for the linear response (LR) of the density of the uniform model system to small perturbations. Similar approaches have been used in classical applications of DFT [38]. The KP $V_{T_s}(\mathbf{r};[\rho])$ can then be readily obtained by functional differentiation. However the exact $T_s[\rho]$ is highly nonlocal, and we have little idea of its functional form for densities far from the linear response regime. It has proved very difficult to understand what errors in the density as determined from the Euler equation with a general $V_{ext}(\mathbf{r})$

will arise from the use of a kinetic potential given by functional differentiation of an approximate nonlocal $T_s[\rho]$.

Conversely, the exact $T_s[\rho]$ can be formally obtained from $V_{T_s}(\mathbf{r};[\rho])$ by a functional integration [6, 25]. Because of this integration over density changes in all regions, $T_s[\rho]$ is a more nonlocal functional of the density than is $V_{T_s}(\mathbf{r};[\rho])$. More detailed arguments arriving at this same conclusion have been presented in a recent article [39]. Since most problems in devising accurate approximations for $T_s[\rho]$ have arisen from the nonlocality, this suggests it could be worthwhile to try to develop approximations for the KP $V_{T_s}(\mathbf{r};[\rho])$ itself. Similar ideas have been successfully used to describe nonuniform classical fluids [40, 41, 42].

Following this line, Chai and Weeks proposed a modified Thomas-Fermi (MTF) KP for atoms [13], by adding a simple gradient correction to the original TF kinetic potential [31], with a coefficient chosen to reproduce the exact boundary condition of exponential decay of the electron density far from the nucleus. This work will be reviewed below in Chap. (3.5) of this thesis. Their results for energies of atoms and for closed-shell diatomic molecules have shown notable success when compared to the original TF and related models, thus indicating that the kinetic potential is indeed a useful quantity to study.

However, the MTF KP does not satisfy the exact LR behavior in the homogeneous limit and the simple local gradient correction used can never reproduce the oscillatory atomic shell structure. It has been argued that appearance of the atomic shell structure is a very sensitive test of the accuracy of $T_s[\rho]$ or $V_{T_s}(\mathbf{r};[\rho])$ [16]. Since only a truly nonlocal KEDF or KP can satisfy the exact LR condition, we have de-

veloped new and more general nonlocal approximations for the KP, as described below. These satisfy the exact linear response condition in the uniform limit, and reproduce the known local limiting forms of the exact $V_{T_s}(\mathbf{r};[\rho])$ both for slowly varying and rapidly varying perturbations. As will become clear, the nonlocality in our KP is completely determined by the requirement that linear response is exactly satisfied. However, even with all these limits satisfied, it would be difficult for our model to give a very accurate description of the large and rapidly varying atomic core electron density. In the next section, we suggest using the more slowly varying valence component of the electron density as described by local pseudopotentials to further reduce the possible remaining errors in our KPs.

1.4 *Ab Initio* Local Pseudopotentials

In most molecular and solid-state applications the inner shell core density changes very little, and most of the interesting physics is associated with changes in the small and more slowly varying valence electron density. Pseudopotential methods have been widely used in molecular and solid-state physics to deal with such problems. In these approaches, the full potential is replaced by a weak pseudopotential acting only on the valence electrons. For OF-DFT, the use of pseudopotentials not only can reduce the computational cost, but also can improve its accuracy. Since most of the nonlocal KEDFs and KPs are based on LR theory, model systems with weak potentials are certainly desirable. However, most of the existing pseudopotentials are orbital-dependent [43, 44, 45], and thus can not be directly applied to

OF-DFT, where the full density is the relevant variable.

Recently, so-called *ab initio* local pseudopotential (AILPS) methods have been developed. In these approaches, given a target valence electron density, the corresponding one-body potential producing that density can be generated by solving the KS equations inversely, because of the one-to-one mapping between density and potentials in DFT [46]. The AILPS is then determined by subtracting the Hartree and the exchange-correlation contributions from the resulting one-body potential. In principle, the AILPS is the unique and exact local potential generating the target density if an exact exchange-correlation energy functional $E_{xc}[\rho]$ is used. It has been shown that even with the simplest local $E_{xc}[\rho]$, good results comparable to those based on nonlocal orbital-dependent pseudopotentials can be obtained [17, 47].

To use this method, an input valence density is needed. In most current work the valence density arising from some standard nonlocal pseudopotential method is used as the target density for generating the AILPS. The above scheme is rather inflexible, since it relies on the existence of an independent pseudopotential calculation, and the associated core electronic configurations are usually chosen to be the noble gas configurations where the subshells are completely filled.

For our purposes here we want to define a valence density component that is small and slowly varying in the core region. This presumably will generate a weak and relatively slowly varying AILPS. This will be more suitable for use in our OF-DFT, which will be most accurate if the system is close to the linear response regime. In Chapter (4.6) below we propose a simple and systematic way to construct such a valence density component and the associated AILPS for atoms. Very promising

results for atomic energies and densities are then found using our OF-DFT, and the AILPS can be used in molecules and solids.

1.5 Outline of the Dissertation

The remainder of this dissertation is organized as follow. Chapter 2 will discuss some general relations connecting the kinetic energy density functional $T_s[\rho]$ and the kinetic potential $V_{T_s}(\mathbf{r};[\rho])$. Chapter 3 will introduce several general and important concepts, such as the limiting forms of the KEDF for slowly varying and rapidly varying perturbations, and discuss linear response (LR) theory, an exact theory for the response of density of the uniform electron gas to small perturbations. Some important earlier work in OF-DFT will also be reviewed in Chapter 3. Our new method is then described in the subsequent chapters. Chapter 4 will develop a family of nonlocal KPs incorporating the correct limiting forms of the exact KP and the exact LR of the free-electron gas, and will propose a simple and systematic scheme to generate a valence density component consistent with a weak and slowly-varying AILPS from the one-to-one mapping between the external potential and the density in DFT. Chapter 5 will compare the numerical results of the present work with the KS-DFT, and other KEDFs. We show that the use of AILPS further reduces errors arising from the nonlocality of an approximate KP or KEDF. Finally, Chapter 6 will review the current situation, and suggest possible directions for future work on OF-DFT.

Chapter 2

Construction of $T_s[\rho]$

2.1 Introduction

If $T_s[\rho]$ is known, $V_{T_s}(\mathbf{r};[\rho])$ can be simply computed by functional differentiation. However, there is no unique way of determining $T_s[\rho]$ from a given $V_{T_s}(\mathbf{r};[\rho])$. Many possible pathways can be used to construct $T_s[\rho]$ by functional integration of $V_{T_s}(\mathbf{r};[\rho])$ using a coupling parameter [48, 49]. Because of this functional integration over density variations in all space, $T_s[\rho]$ is a more nonlocal functional of the density than is $V_{T_s}(\mathbf{r};[\rho])$ [13]. If the exact $V_{T_s}(\mathbf{r};[\rho])$ is used in the integration, then all pathways would give the same exact result for $T_s[\rho]$. However, when an approximate $V_{T_s}(\mathbf{r};[\rho])$ is used, different pathways will give different results for the kinetic energy. However, this "thermodynamic inconsistency" is small if reasonably good approximations for the density are used, since the integration tends to average out local errors in the density [13]. Here, we discuss three important pathways.

2.2 Herring's Pathway

There is a particular pathway [6, 25] arising from exact scaling relations between the non-interacting kinetic energy $T_s[\rho]$ with respect to the coordinate $\mathbf{r}$ in $\rho(\mathbf{r})$ where very simple results involving only the final density can be found. If the coor-

dinate $\mathbf{r}$ is scaled to $\alpha\mathbf{r}$, the normalized scaled density is $\rho_\alpha(\mathbf{r}) = \alpha^3\rho(\alpha\mathbf{r})$. The corresponding normalized scaled KS orbitals in Eq. (1.8) become $\psi_{i,\alpha}(\mathbf{r}) = \alpha^{3/2}\psi_i(\alpha\mathbf{r})$. The exact $T_s[\rho_\alpha]$ in Eq. (1.9) then obeys

$$\begin{aligned} T_s[\rho_\alpha] &= \sum_i \int \psi_{i,\alpha}(\mathbf{r})(-\frac{\bigtriangledown^2}{2})\psi_{i,\alpha}(\mathbf{r})d\mathbf{r} = \sum_i \int \alpha^{3/2}\psi_i(\mathbf{x})(-\frac{\alpha^2\bigtriangledown_{\mathbf{x}}{}^2}{2})\alpha^{3/2}\psi_i(\mathbf{x})(\alpha^{-3}d\mathbf{x}) \\ &= \alpha^2 \sum_i \int \psi_i(\mathbf{x})(-\frac{\bigtriangledown_{\mathbf{x}}{}^2}{2})\psi_i(\mathbf{x})d\mathbf{x} \\ &= \alpha^2 T_s[\rho] \end{aligned} \tag{2.1}$$

where $\bigtriangledown_x^2$ is the Laplacian with respect to the coordinate $\mathbf{x} \equiv \alpha\mathbf{r}$.

For isolated systems, such as atoms and molecules, the density and its derivatives to all order vanish far from the nuclei. For such systems, when Eq. (2.1) is differentiated with respect to α, and the partial derivative is evaluated at $\alpha = 1$, boundary terms vanish and we find the formally exact result

$$T_s[\rho] = \frac{1}{2}\int V_{T_s}(\mathbf{r};[\rho])\bigtriangledown\cdot(\mathbf{r}\rho(\mathbf{r}))d\mathbf{r}. \tag{2.2}$$

Therefore, once the kinetic potential $V_{T_s}(\mathbf{r};[\rho])$ is known for some given $\rho(\mathbf{r})$, the numerical value of $T_s[\rho]$ can then be immediately determined. Since there is no need to perform a coupling parameter integration over the change of density or potential, this scheme is not only fast, but also numerically reliable. The final form of Eq. (2.2) is essentially the viral theorem of Clausius, and is directly related to the force on molecules [50, 51, 52, 53]. Since this pathway was first derived by Herring, we refer to it as the Herring's pathway.

Note that this simple and exact pathway holds only for the *noninteracting*

$T_s[\rho]$ [52], which again shows the virtues of the KS partitioning of the total energy. We will use Eq. (2.2) as the basic pathway to determine the numerical value of $T_s[\rho]$ from a given approximate $V_{T_s}(\mathbf{r};[\rho])$ for all calculations for isolated systems in this dissertation. Other pathways can be used to check the accuracy of the V_{T_s}, since results using the exact V_{T_s} would be independent of path [48, 49]. For extended systems, Eq. (2.2) does not hold because of nonvanishing boundary terms. Thus far we have not found an exact and simple way of including them, though we think this remains a promising line for future research. In the following sections we discuss different pathways to determine $T_s[\rho]$ for extended systems.

2.3 Density Pathway

The change in the kinetic energy can be formally related to a coupling parameter integration, where the density changes from some known value at $\lambda = 0$ to the final density at $\lambda = 1$:

$$T = T_{\lambda=0} + \int_0^1 d\lambda \int d\mathbf{r} V_{T_s}(\mathbf{r};[\rho_\lambda]) \frac{\partial \rho_\lambda(\mathbf{r})}{\partial \lambda} \tag{2.3}$$

For the linear density pathway, the density $\rho(\mathbf{r})$ is linearly scaled by a coupling parameter λ

$$\rho_\lambda(\mathbf{r}) = \rho_0 + \lambda[\rho(\mathbf{r}) - \rho_0] \tag{2.4}$$

where ρ_0 is some uniform reference density, naturally chosen to be the uniform electron density N/V in extended systems.

When Eq. (2.4) is differentiated with respect to λ, it gives

$$\frac{\partial \rho_\lambda(\mathbf{r})}{\partial \lambda} = \rho(\mathbf{r}) - \rho_0 \tag{2.5}$$

Inserting Eqs. (2.4 ,2.5) into Eq. (2.3), we have

$$T = T_{\lambda=0} + \int_0^1 d\lambda \int d\mathbf{r} V_{T_s}(\mathbf{r}; [\rho_\lambda])[\rho(\mathbf{r}) - \rho_0] \tag{2.6}$$

As can been seen in Eq. (2.6), in order to obtain the value of kinetic energy T from this density pathway, knowledge of $T_{\lambda=0}$ is needed. Since one takes the uniform system as the reference system ($\lambda = 0$), $T_{\lambda=0}$ is the kinetic energy of the uniform system, which is exactly the Thomas-Fermi kinetic energy $T_{TF}[\rho]$ with $\rho(\mathbf{r}) = \rho_0 = N/V$ the uniform electron density. For extended systems, where the Herring's pathway fails, this density pathway appears to be a good way to compute T. Other density pathways can be defined, and have proved useful in certain applications, like the square-root pathway introduced by Chen and Weeks [49] to describe nonuniform hard sphere fluids,

$$\rho_\lambda^{1/2}(\mathbf{r}) = \rho_0^{1/2} + \lambda[\rho^{1/2}(\mathbf{r}) - \rho_0^{1/2}] \tag{2.7}$$

We expect very little path dependence for all such density pathways, since the difference between kinetic energy of the real system (T), and the reference system ($T_{\lambda=0} = T_{TF}[\rho] \mid_{\rho(\mathbf{r})=\rho_0}$) is expected to be relatively small, and the KP contributes only to this small term. Furthermore, from Eq. (2.3), $\rho_\lambda(\mathbf{r})$ is the only λ-dependent term, and depends only on the final density. Thus unlike other coupling parameter approaches where the potential is scaled (described in the next section) [48, 49],

there is no need to solve the Euler equation (1.3) for its corresponding external potential $V_{ext}^{\lambda}(\mathbf{r})$ at each λ-value (with the same μ). Therefore, this pathway is computationally efficient. However, for isolated systems, where $\rho_0 = 0$, this pathway is likely to be less accurate than the Herring's pathway, since it does not satisfy the virial theorem.

2.4 Potential Pathway

Instead of computing the kinetic energy directly, or with a density pathway, one can compute the total energy by using a coupling parameter approach [13, 48, 54] to scale the external potential. The kinetic energy can then be found by subtracting the potential energy (calculated from the potential energy density functionals) from the total energy. This pathway is, however, considerably more expensive than the density pathway, since one needs to solve the Euler equation (1.3) for each $V_{ext}^{\lambda}(\mathbf{r})$ (with the same μ), to determine the corresponding ρ_{λ}. A detailed description of this pathway is given in Chapter 3.

2.5 Summary

To sum up, for isolated systems, the Herring's pathway is most appealing, due to its satisfaction of the virial theorem, and will be used in this dissertation. For extended system, where Herring's pathways fails, the density pathway is most attractive. One can also use the potential pathway as a check for the possible pathway dependence of the KPs.

Chapter 3

Exact Limits and Earlier Work

3.1 Slowly Varying Limits

Although the exact $T_s[\rho]$ is still unknown, several limiting forms have been discovered for particular density distributions. We discuss results for the KEDFs here; results for the associated kinetic potentials follow immediately by functional differentiation and will be used in Chapter 4. In particular, the TF KEDF from Eq. (1.10), is known to be exact for a uniform system [31]. Results for nonuniform systems are best described in Fourier space. For a slowly varying perturbation of the density, one might try to improve the TF model by including gradients of the density.

Based on the $\hbar$ expansion of single-electron Green's function to $O(\hbar^2)$, the correct second order gradient expansion correction to the TF KEDF is known [55], and is reproduced by using only 1/9 of the original von Weizsäcker correction in Eq. (1.11):

$$T_{TF\frac{1}{9}W}[\rho] \equiv T_{TF}[\rho] + \frac{1}{9}T_W[\rho]. \tag{3.1}$$

There have been considerable efforts to develop gradient expansions to higher orders [56, 57, 58, 59]. At present, the highest order gradient expansion with an analytic form is the sixth order [59]. However, for isolated systems, where density decays exponentially, these KEDFs are divergent at sixth and higher order, and

the KPs are divergent at fourth order and higher. Here, we limit our discussion to the second order expansions, since the TF1/9W model does not have the above problems, and can be applied to both isolated and extended systems. However, it is not very accurate in practice, and serves as only one of the limits our models will obey.

3.2 Rapidly Varying Limits

On the other hand, for a rapidly varying perturbation with only high wavevector components, the W KEDF $T_W[\rho]$ from Eq. (1.11) is the leading term [35]. Moreover, this is known to be exact for a system with one or two electrons, or where the density can be accurately described by a single orbital [1]. Results correct to second order at high wavevectors [14, 15, 16, 19] are reproduced by

$$T_{W-\frac{3}{5}TF}[\rho] \equiv T_W[\rho] - \frac{3}{5}T_{TF}[\rho]. \tag{3.2}$$

3.3 Linear Response Theory

Finally, the linear response of the density of a uniform non-interacting electron gas with density ρ_0 to a small perturbation $\delta V(\mathbf{k}) = \epsilon_{\mathbf{k}} e^{i\mathbf{k}\cdot\mathbf{r}}$ is exactly known [60],

$$\delta\rho(\mathbf{k}) = \chi_L(q)\delta V(\mathbf{k}). \tag{3.3}$$

The LR function $\chi_L(q)$ for the uniform electron gas can be written in terms of a dimensionless wavevector

$$q \equiv k/2k_F, \tag{3.4}$$

where

$$k_F \equiv (3\pi^2\rho_0)^{1/3} \tag{3.5}$$

is the Fermi wavevector (FWV) and $k \equiv |\mathbf{k}|$. $\chi_L(q)$ has the form

$$\begin{aligned} \chi_L(q) &= -\frac{k_F}{\pi^2} F_L^{-1}(q) \\ &= -\frac{k_F}{\pi^2}\left[\frac{1}{2} + \frac{1-q^2}{4q}\ln\left|\frac{1+q}{1-q}\right|\right], \end{aligned} \tag{3.6}$$

where

$$F_L(q) \equiv \left[\frac{1}{2} + \frac{1-q^2}{4q}\ln\left|\frac{1+q}{1-q}\right|\right]^{-1} \tag{3.7}$$

has been called the Lindhard function [16].

It is known that the weak logarithmic singularity at $q = 1$ in $F_L^{-1}(q)$ is responsible for Friedel oscillations, and may also be important for the appearance of atomic shell structure. This singularity further divides the Lindhard function into two branches in Fourier space: the low-momentum ($q < 1$) or the low-q (LQ) branch, and the high-momentum ($q > 1$) or the high-q (HQ) branch [16].

By linearization of the TF and W KPs, the corresponding dimensionless response function for the TF KEDF is $F_{TF}(q) = 1$, and that for the W KEDF is $F_W(q) = 3q^2$ [61]. Clearly, no linear combination of the TF and the W KEDFs can reproduce the exact Lindhard function in Eq. (3.7). This has the following two limits [16],

$$F_L(q) = \begin{cases} 1 + \frac{q^2}{3} + O(q^4) & q \ll 1 \\ 3q^2 - \frac{3}{5} + O(q^{-2}) & q \gg 1 \end{cases} \tag{3.8}$$

For $q \ll 1$, $F_L(q)$ reduces to the LQ limit, where the first (leading) term is from the TF KEDF, and the second term is from the second-order gradient correction in Eq. (3.1). For $q \gg 1$, $F_L(q)$ reduces to the HQ limit, where the leading term is from the W KEDF, and the second term is due to the second-order high wavevector expansion in Eq. (3.2).

It should be noted that the expressions for both the low-q and high-q limits are correct to all orders in perturbation theory, but valid only in the appropriate limits in Fourier space. On the other hand, the LR theory is valid for all wavevectors, but is only accurate for small perturbations. Therefore, the range of wavevectors where the response functions of the two limiting KEDFs deviate from the exact LR function gives an indication of the regimes where the two limiting forms are inaccurate.

In summary, although the exact $T_s[\rho]$ or $V_{T_s}(\mathbf{r};[\rho])$ are still unknown, knowledge of the existing limiting forms of the exact KEDF at large and small wavevectors and the exact LR theory in the homogeneous limit provides important cornerstones for constructing accurate KEDFs and KPs, as will be seen below. In the next Section we review previous attempts to construct KEDFs and our earlier work on the KP for the MTF model.

3.4 Kinetic Energy Density Functionals $T_{TF\lambda W}[\rho]$ and $T_{W\lambda TF}[\rho]$

Since $T_{TF}[\rho]$ and $T_W[\rho]$ are the only ingredients in the two limiting forms of the exact $T_s[\rho]$ up to second order, simple linear combinations of these two KEDFs,

such as the TFλW KEDF [32, 36, 55, 62]

$$T_{TF\lambda W}[\rho] \equiv T_{TF}[\rho] + \lambda T_w[\rho] \tag{3.9}$$

and the WλTF KEDF [63, 64, 65, 66]

$$T_{W\lambda TF}[\rho] \equiv T_W[\rho] + \lambda T_{TF}[\rho] \tag{3.10}$$

have been widely studied for several decades. The value of the parameter λ was either determined empirically for getting good atomic energies or obtained by some semiclassical arguments. For example, the TF1/9W KEDF, as discussed before, has been shown to give the correct second order gradient expansion correction to the TF functional and to reproduce the exact linear response of a homogeneous electron gas under a long wavelength perturbation [55], but energy predictions for atoms are inaccurate; the TF1/5W KEDF, found empirically by Tomishima and Yonei [62], predicts rather accurate atomic ground state energies for a wide range of Z. The advantage of these approaches is the ability to generate a family of simple KEDFs easily. The $T_{TF\lambda W}[\rho]$ and $T_{W\lambda TF}[\rho]$ give the correct leading term in the density response to a slowly-varying perturbation and a rapidly-varying perturbation respectively, although they have the incorrect leading term in the opposite limit, unless $\lambda = 1$. However, it has been shown that $T_{TFW}[\rho]$ with $\lambda = 1$ always overestimates the exact $T_s[\rho]$ for various systems [16]. Finally, neither the response function of the TFλW KEDF ($F_{TF\lambda W}(q) = 1 + 3\lambda q^2$) nor that of the W$\lambda$TF KEDF ($F_{W\lambda TF}(q) = 3q^2 + \lambda$) can reproduce the exact response function $F_L(q)$ in the homogeneous limit.

Although some of these approaches can provide accurate predictions for atomic energies, the predicted density profiles are generally not very accurate, both near and far away from the nucleus. Since these models fail to satisfy the known limiting forms, and nonlocality in $T_s[\rho]$ is not correctly described, it is also not surprising to see that atomic shell structure is missing in these approaches.

3.5 Modified Thomas Fermi Kinetic Potential

This section is heavily based on a published paper by J.-D. Chai and J. D. Weeks, *Journal of Physical Chemistry* B **108**, 6870 (2004).

3.5.1 Modified Euler Equations for the Density Response

As argued above, it may be more profitable to examine simple gradient corrections directly in the more local Euler equation. The Euler equation arising from use of the TFλW expression for $T_s[\rho]$ is

$$\mu = V_{TF}(\mathbf{r};[\rho]) + \frac{\lambda}{8}\frac{|\nabla\rho(\mathbf{r})|^2}{\rho(\mathbf{r})^2} - \frac{\lambda}{4}\frac{\nabla^2\rho(\mathbf{r})}{\rho(\mathbf{r})} + V_{eff}(\mathbf{r}) \tag{3.11}$$

There is a local term in the density from the TF model

$$V_{TF}(\mathbf{r};[\rho]) \equiv \delta T_{TF}[\rho]/\delta\rho(\mathbf{r}) = \frac{5}{3}C_F\rho^{2/3}(\mathbf{r}), \tag{3.12}$$

and *two* terms involving density gradients from the W model

$$V_W(\mathbf{r};[\rho]) \equiv \delta T_W[\rho]/\delta\rho(\mathbf{r}) = \frac{1}{8}\left(\frac{|\bigtriangledown\rho(\mathbf{r})|^2}{\rho(\mathbf{r})^2} - 2\frac{\bigtriangledown^2\rho(\mathbf{r})}{\rho(\mathbf{r})}\right). \tag{3.13}$$

Both terms must be present with specified coefficients if we insist on using simple local expressions of the von Weizsäcker form directly in $T_s[\rho]$ with no compensating terms from nonlocal corrections. However the first nonlinear gradient term does not have a simple physical interpretation and does not appear in the analogous classical van der Waals equation for the liquid-vapor interface [40]. A linear gradient correction like the second term would be expected on quite general grounds. Moreover we find that the second term alone is responsible for producing a finite density at an atomic nucleus with $V_{ext}(\mathbf{r}) = V_{ext}(r) = -Z/r$, effectively building in the uncertainty principle, and of course this term alone contributes to the linear response of the density to weak fields. Finally this term yields exponential decay far from the nucleus.

Thus we propose as the simplest correction to the TF kinetic potential a modified Euler equation where only the linear gradient term appears, with a coefficient chosen to best describe the density response. To avoid confusion in notation, λ is changed to α in our new Euler equation:

$$\mu = V_{TF}(\mathbf{r};[\rho]) - \frac{\alpha}{4}\frac{\nabla^2\rho(\mathbf{r})}{\rho(\mathbf{r})} + V_{eff}(\mathbf{r}). \tag{3.14}$$

Note that we use a $V_{eff}(\mathbf{r})$ that includes the effects of exchange and correlation in all the calculations reported herein. Thus Eq. (3.14) does not reduce to the classical TF model when $\alpha = 0$.

We first examine the predictions of this model for atoms. It is easy to show that the density at the nucleus is finite for any choice of α and satisfies

$$\frac{\rho'(0)}{\rho(0)} = -\frac{2Z}{\alpha}. \tag{3.15}$$

The exact cusp condition [67] for the logarithmic derivative of the density at the origin can be satisfied if $\alpha = 1$, as in the TFW model. However this choice does not guarantee correct values for $\rho(0)$ and $\rho'(0)$ separately, and indeed the TFW model gives very poor results for these terms. For example, for Ar $\rho(0)$ is 72% below the HF value. Moreover the nonlinear gradient term in the TFW model does not seem to improve the density at intermediate values of r when compared to the results of our model.

Equation (3.14) also produces exponential decay of the density at large r, where

$$\rho(r) \approx \exp[-(-4\mu/\alpha)^{\frac{1}{2}} r]. \tag{3.16}$$

When $\alpha = 1/2$, the correct exponential decay constant for the exact μ is predicted.

Using this one parameter model we cannot satisfy both the exact cusp condition and asymptotic decay condition with the same α, and it is clear that no oscillatory shell structure will be generated by the simple gradient term. (As is the case for the classical van der Waals theory of interfaces, nonlocal corrections are required to get oscillatory structure [40].) But we can hope that a proper choice of α could give a smoothed electron density that reproduces important overall features and gives improved atomic energies when compared to the TF model. Since any α produces a finite density at the nucleus and thus corrects a major shortcoming of the TF model, we choose $\alpha = 1/2$ to give the correct exponential decay of the density far from the nucleus. This is the region that should be most important in chemical bonding. In the following we refer to Eq. (3.14) with $\alpha = 1/2$ as the

modified Thomas-Fermi (MTF) model [13]:

$$V_{MTF}(\mathbf{r};[\rho]) = V_{TF}(\mathbf{r};[\rho]) - \frac{1}{8}\frac{\bigtriangledown^2\rho(\mathbf{r})}{\rho(\mathbf{r})}. \tag{3.17}$$

We show below that the MTF model gives atomic energies comparable to those of the best TFλW model with $\lambda = 1/5$ along with a much better description of the density distribution.

3.5.2 Results for the MTF Model

Linear Response Function

We first examine the predictions of the various models for the linear response of the density of the model system to a weak perturbing potential. It is easy to see that the nonlinear gradient term in Eq. (3.11) does not contribute to the linear response function of the TFλW models ($F_{TF\lambda W}(q) = 1 + 3\lambda q^2$). As a result, the linear response function for the MTF model, derived from Eq. (3.14) with $\alpha = 1/2$, is the same as the TF$\frac{1}{2}$W model.

As shown in Fig. (3.1), the response function of $T_{TF}[\rho]$ ($F^{-1}_{TF}(q)$) is only exact at $q = 0$, and has no momentum dependence, while the response function of $T_{TF\frac{1}{9}W}[\rho]$ ($F^{-1}_{TF\frac{1}{9}W}(q)$) remains accurate for $q < 0.5$, but decays very slowly as $q \to \infty$. The LR function of $T_W[\rho]$ ($F^{-1}_W(q)$) is exact asymptotically at high q, and remains accurate for $q \gtrsim 2$. The LR function of $T_{W-\frac{3}{5}TF}[\rho]$ ($F^{-1}_{W-\frac{3}{5}TF}(q)$) remains accurate for $q \gtrsim 1.2$, and has a larger valid regime than $T_W[\rho]$. However, both $F^{-1}_W(q)$ and $F^{-1}_{W-\frac{3}{5}TF}(q)$ are divergent in the low-q branch, and fail completely for the nearly uniform electron gas. In contrast, the MTF model gives a reasonable

Figure 3.1: Linear response functions of a uniform system of noninteracting Fermions as given by the various models.

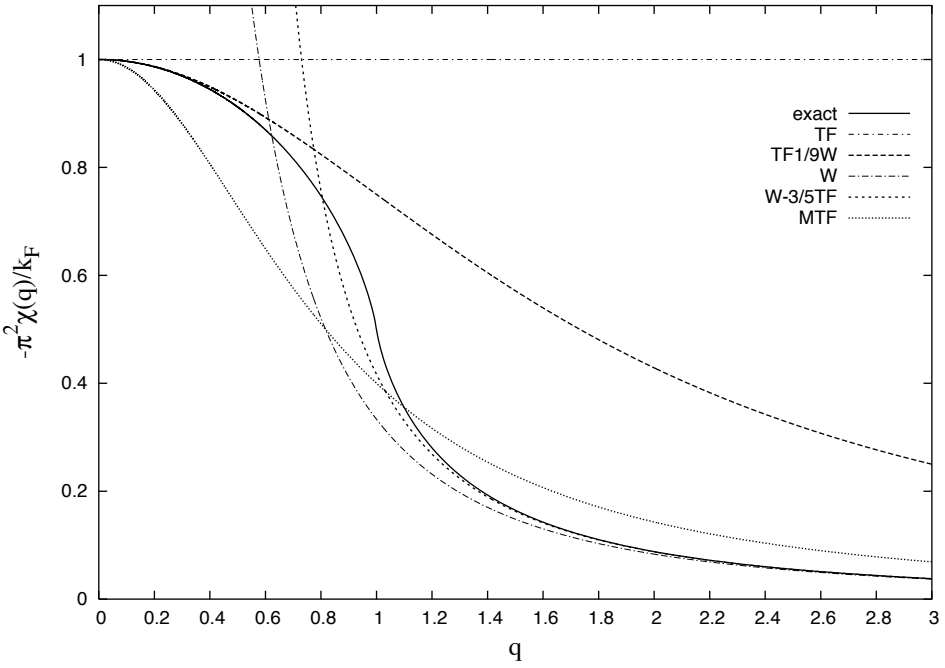

average description of the exact response function, especially in the important region near the singularity at $q = 1$.Wang *et al.* [16] have suggested that reproducing the singularity and the overall form of the linear response function are important for obtaining the correct physics from OF methods, particularly for producing the shell structure of atoms. While no simple gradient type model can describe the singularity exactly (or give shell structure), the MTF model captures the average behavior of the linear response function and shows better accuracy in the physically significant region near $q = 1$.

Atoms

We carried out benchmark calculation on the hydrogen atom and the rare gas atoms based on our MTF model. Our results are compared with the TF model, and its von Weizsäcker-type gradient corrections. We examined $\lambda = \frac{1}{9}, \frac{1}{5}, \frac{1}{2}$, and 1 but report results only for $\lambda = \frac{1}{5}$ and 1, and for the KS and HF methods. The local density approximation (LDA) [68, 69, 70] for the exchange-correlation functional is used for all the models. The standard method for solving Euler equations derived from the TFλW model [71] was implemented to solve the Euler equation for the MTF model and the KS theory. Our TF$\frac{1}{5}$W and KS results are in very good agreement with previous calculations [72] using a slightly different LDA parameterization [73]. The code uses the finite difference method with the Gauss-Chebyshev (of the second kind) radial quadrature, proposed by Becke *et al.*, consisting of 1000 points, and Becke's algorithms for solving Poisson's equation for the Hartree potential [74].

As shown in Table 3.1, the electron density at the nucleus, $\rho(0)$, calculated by the MTF model is close to the HF results from Clementi *et al* [75]. As discussed above, the TF model predicts an infinite value for the electron density, while the TF$\frac{1}{5}$W models overestimates the density by a factor of 4. The TFW model considerably underestimates the density, despite satisfying the exact cusp condition. It is known [76] that $\rho(0)$ is related to the density moments $\langle r^{-1} \rangle$ and $\langle r^{-2} \rangle$. Thus the MTF model would be expected to give good results for these expectation values, as is shown in Table 3.2 and 3.3 respectively, when compared with the KS and HF result*s* [77].

In Table 3.4 we compare the chemical potential μ for the MTF theory, calculated by a self-consistent solution of Eq. (3.14), with that given by the KS equation and find very good agreement. This means that the asymptotic behavior of the density predicted by the MTF model is close to the prediction of the KS theory, since the MTF model would give exact results for the exact μ. Since the accuracy of the density in the tail is an important indicator of chemical bonding [1], we believe that this desired behavior could lead to chemical bonding in molecules.

The Euler equation (3.14) for the MTF model is not derived by a functional derivative of an energy functional. As a result we cannot immediately obtain the energy once we have determined the density, as would be possible in OF methods that give direct approximations for $T_s[\rho]$. Instead, we can use a coupling parameter approach [48, 54] to calculate the energy change as the external potential is turned on:

$$E = E_{\lambda=0} + \mu \int [\rho_{\lambda=1}(\mathbf{r}) - \rho_{\lambda=0}(\mathbf{r})] d\mathbf{r} + \int_0^1 d\lambda \int \rho_\lambda(\mathbf{r}) V_{ext} d\mathbf{r} \tag{3.18}$$

Here the external potential V_{ext} is linearly scaled by a coupling parameter λ (not to be confused with the λ parameter in the TFλW methods) and the corresponding density is ρ_λ. E is the total energy of the system, and $E_{\lambda=0}$ is the total energy at the same μ in the absence of the external potential.

If exact values for ρ_λ were used, Eq. (3.18) would give exact results and a variety of different integration pathways (e.g., nonlinear scaling of V_{ext}) could be used. Since we make approximations there will be errors in our predicted E values and different pathways could (incorrectly) give different results. However,

our experience for the analogous classical problem suggests that these errors are small if the density is reasonably accurate [49], as seems to be the case here.

We note that $\rho_{\lambda=0}$ and thus $E_{\lambda=0}$ vanish for the uniform electron gas because of the fixed negative value of the chemical potential. Therefore, E, the total energy, can be straightforwardly computed from Eq. (3.18) by numerical integration over a series of λ values. For the benchmark calculations reported here for the total energy, 1000 points are used between $\lambda = 0$ and $\lambda = 1$, though reasonable results can be obtained with about 10 points. The kinetic energy can then be found by subtracting the potential energy (calculated from the potential energy density functionals) from the total energy. This way of obtaining kinetic energy is equivalent to integrating the kinetic potential directly as discussed above, but we believe it is numerically more accurate. We also check the possible pathway dependence of the MTF KP by using the Herring's pathway (see Eq. (2.2)). As shown in Table 3.5, the total energy of the MTF model is comparable to that of the TF$\frac{1}{5}$W model, the best TFλW model for the total atomic energy.

In Figs. (3.2 – 3.5), we compare the radial density distribution $r^2\rho(r)$ of the MTF model to that predicted by other theories. Although the MTF model shows no shell structure when compared to the essentially exact KS theory, it gives a nice averaging of the electron density, with slightly more emphasis on the principle peak than in the TFλW models, along with significantly better results both near and far from the nucleus. The fact that a smooth density can give such accurate energies illustrates the point that the integration in Eq. (3.18) renders it less sensitive to small errors in the density. As can also been seen, the difference of total energy

Figure 3.2: Radial density $r^2\rho$ of the Neon atom with the various TF-type models, the KS method, and the MTF model.

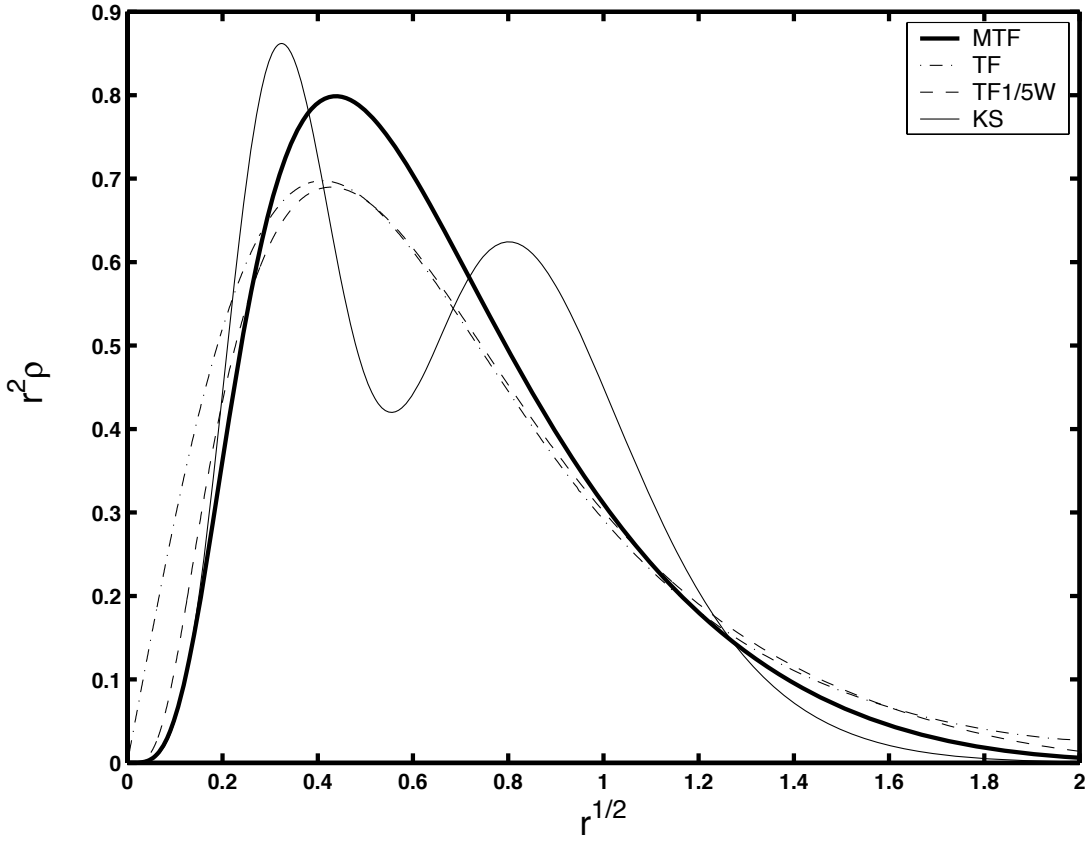

Figure 3.3: Same as in Fig. (3.2) but for the Argon atom

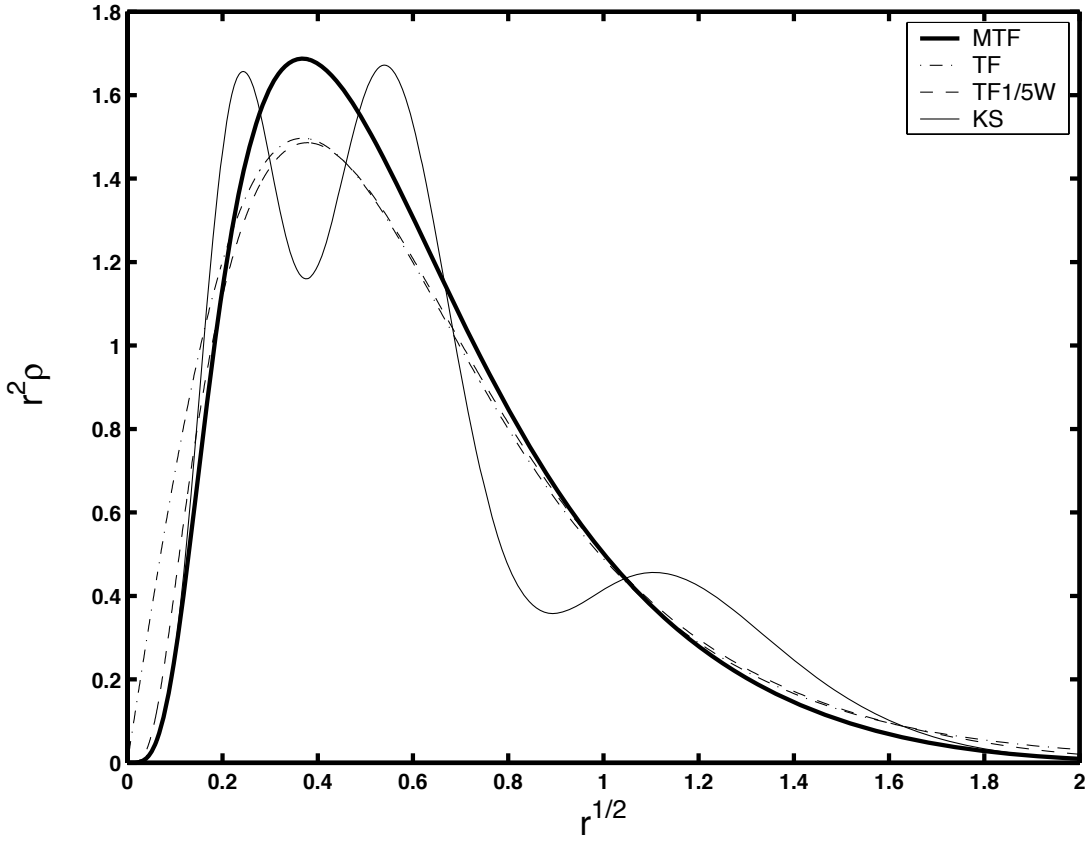

Table 3.1: Electron density at the nucleus $\rho(0)$ using the various TF-type models, the KS method, the HF method and the MTF model. The HF data is taken from Clementi *et al* [75].

	MTF	HF	$TF\frac{1}{5}W$	TFW	KS
H	0.5820	0.3183	2.390	0.1029	0.2728
He	5.208	3.596	19.29	0.9515	3.525
Ne	788.2	619.9	2595	169.6	614.5
Ar	4811	3840	15482	1093	3819
Kr	40064	32236	126491	9579	32146
Xe	137631	112219	431005	33710	111005

Figure 3.4: Same as in Fig. (3.2) but for the Krypton atom

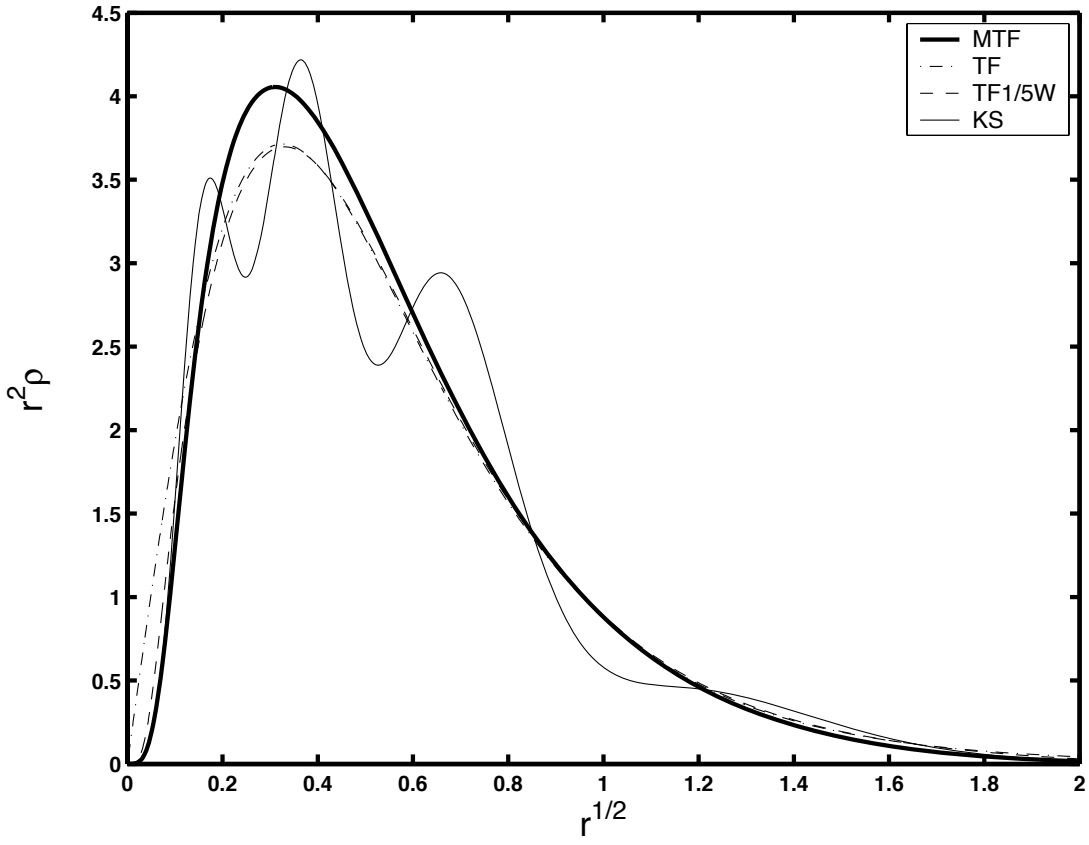

Table 3.2: $\langle r^{-1} \rangle$ using the TF$\frac{1}{5}$W model, the KS method, and the MTF model.

	MTF	$TF\frac{1}{5}W$	KS
H	1.000	1.249	0.9208
He	2.907	3.261	3.312
Ne	30.56	30.75	31.00
Ar	69.93	69.63	69.62
Kr	183.5	181.7	182.7
Xe	321.2	317.8	317.8

Figure 3.5: Same as in Fig. (3.2) but for the Xenon atom

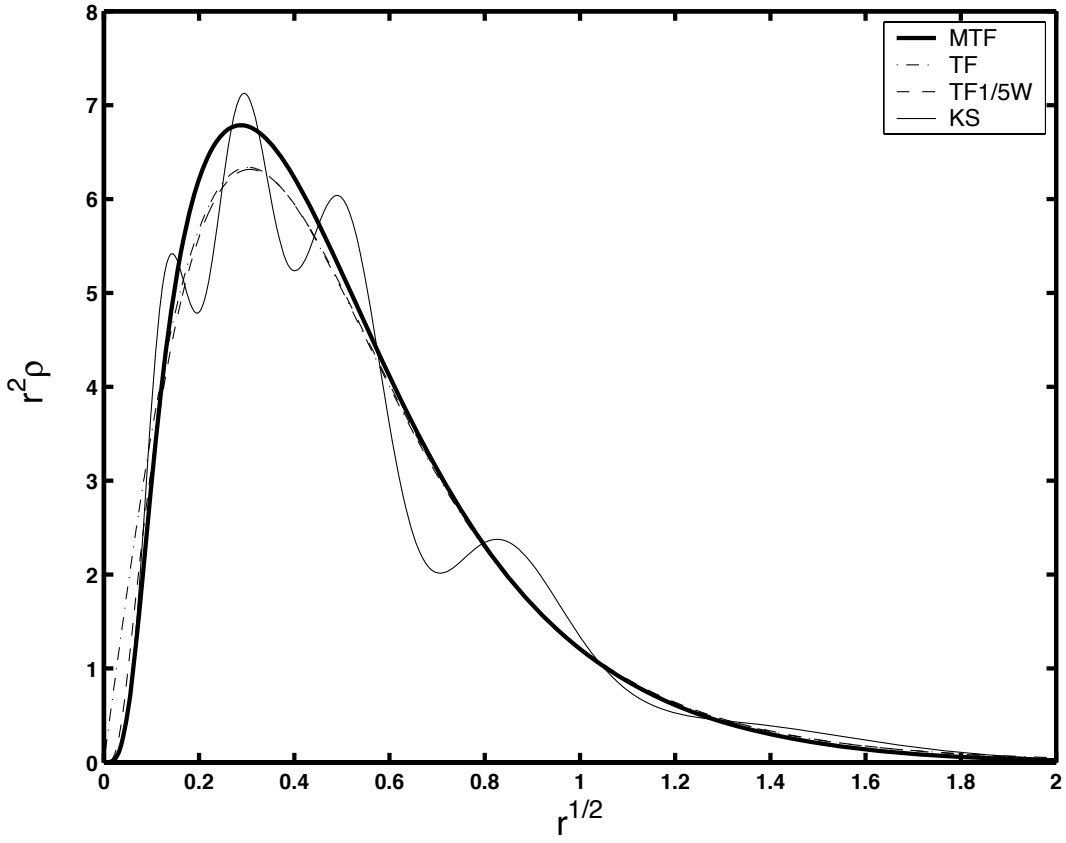

Table 3.3: $\langle r^{-2} \rangle$ using the TF$\frac{1}{5}$W model, the KS method, the HF method, and the MTF model. The HF data is taken from Porras *et al* [77].

	MTF	$TF\frac{1}{5}W$	KS	HF
H	2.394	4.720	1.749	–
He	11.50	20.06	11.71	11.99
Ne	394.7	599.7	411.9	414.9
Ar	1390	2056	1459	1465
Kr	6025	8705	6318	–
Xe	14101	20148	14799	14818

Table 3.4: Atomic chemical potential μ using the various TF-type models, the KS method, and the MTF model.

	MTF	TF	$TF\frac{1}{5}W$	TFW	KS
H	-0.2825	-0.08039	-0.09549	-0.09773	-0.2337
He	-0.3822	-0.06290	-0.1013	-0.1393	-0.5702
Ne	-0.4400	-0.04959	-0.1093	-0.2188	-0.4978
Ar	-0.4304	-0.05034	-0.1112	-0.2346	-0.3823
Kr	-0.4224	-0.05017	-0.1130	-0.2485	-0.3464
Xe	-0.4192	-0.05034	-0.1138	-0.2552	-0.3100

Table 3.5: Atomic energy E using the various TF-type models, the KS method, and the MTF model (evaluated by both the potential and the Herring's pathways).

	MTF_{pot}	MTF_H	TF	$TF\frac{1}{5}W$	TFW	KS
H	-0.6092	-0.4822	-1.076	-0.6085	-0.2927	-0.4459
He	-2.902	-2.547	-4.756	-2.917	-1.559	-2.834
Ne	-129.5	-125.3	-176.6	-129.5	-86.40	-128.2
Ar	-529.0	-517.4	-681.1	-526.2	-375.5	-525.9
Kr	-2774	-2734	-3378	-2747	-2099	-2750
Xe	-7293	-7210	-8643	-7214	-5701	-7229

from these two different pathways is relatively small.

Diatomic Molecules

Gordon and Kim (GK) suggested a simple model for calculating the intermolecular potential of closed-shell molecules [78]. By assuming the molecular density of a diatomic molecule can be expressed as the sum of the two separate atomic densities, reasonable bonding potentials for closed-shell molecules can be obtained. Instead of using the inaccurate TF atomic densities, GK used the atomic HF densities and inserted these into the original TF kinetic energy functional, together with the classical electron-electron and nuclear-electron potentials, and a local density approximation for the exchange-correlation functionals.

We followed GK's simple approach, using atomic densities for the Ar atom given by the various models discussed here. Becke's atomic partition, the Gauss-Chebyshev (of the second kind) radial quadrature, and the Clenshaw-Curtis angular quadrature with 1000 radial points and 500 angular points are used in the numerical calculations [79, 80].

We found that the KS bonding potential is very similar to the HF result, as is expected due to the high quality of its atomic density. As we can see in Fig. (3.6), the strength of the bonding of the TFλW models increases as λ increases. However, the bonding energy is consistently overestimated, even for the smallest value of λ. The MTF model predicts a reasonable bonding curve, with both its strength and bond length close to the HF and KS methods. Note that even the TF density can

Figure 3.6: Ar-Ar interaction potential via the Gordon-Kim approach.

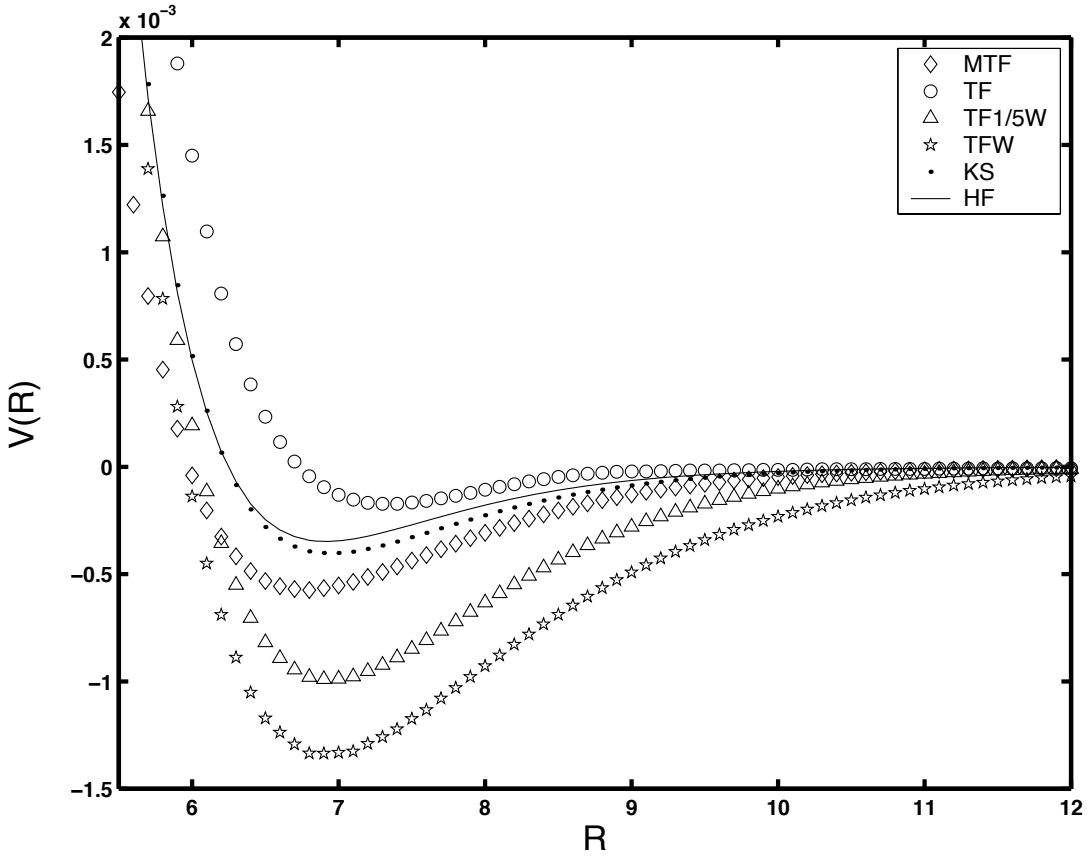

give a qualitatively accurate bonding curve using the GK method, though a self-consistent solution of the molecular density using the TF model is known to give no bonding [33].

3.5.3 Possible Generalizations

We used heuristic arguments to suggest the form of the MTF equation (3.14). One might hope that a more systematic search using generalized forms of this kind could yield even better results. Since the MTF model has only one parameter, α, we considered one such generalization of the gradient term in Eq. (3.14) that allows for the introduction of a second parameter, β, and that interpolates between the MTF and the TFλW models:

$$-\frac{\alpha}{4}\frac{\nabla^2\rho^\beta}{\rho^\beta} = -\frac{\alpha}{4}\left\{\beta(\beta-1)\frac{|\nabla\rho(\mathbf{r})|^2}{\rho(\mathbf{r})^2} + \beta\frac{\nabla^2\rho(\mathbf{r})}{\rho(\mathbf{r})}\right\}. \tag{3.19}$$

For $\alpha = 1/2$ and $\beta = 1$, this reduces to the MTF form, while the TFλW models correspond to $\{\alpha, \beta\} = \{2\lambda, 1/2\}$, as can be seen from Eq. (3.11).

Using this generalized form in Eq. (3.14) for atomic systems, the density at the nucleus is finite and satisfies a modified cusp condition

$$\frac{\rho'(0)}{\rho(0)} = -\frac{2Z}{\alpha\beta}. \tag{3.20}$$

When $\alpha\beta = 1$, the exact cusp condition is satisfied. This form also produces an exponentially decaying density in the tail, satisfying

$$\rho(r) \approx \exp\left[-\left(\frac{-8\mu}{2\alpha\beta^2}\right)^{\frac{1}{2}} r\right]. \tag{3.21}$$

When $2\alpha\beta^2 = 1$ the correct asymptotic decay constant is found for the exact μ.

However only when $\{\alpha, \beta\} = \{2, 1/2\}$ (i.e., the original von Weizsäcker model with $\lambda = 1$) can both conditions be satisfied simultaneously. Since all values give a finite density at the origin, we also considered the one parameter family of models with $2\alpha\beta^2 = 1$ that give the correct exponential decay constant. However, the best overall results for the atomic energy and density were still found using the MTF model with $\{\alpha, \beta\} = \{1/2, 1\}$. Evidently the nonlinear gradient term in Eq. (3.19) that is generated when $\beta \neq 1$ does not improve the simple MTF model and other forms should be examined.

3.5.4 Final Remarks

In summary of our previous work, using the simple KP of Eq. (3.17), one can get agreement of the atomic energy and chemical potential comparable to the best TFλW models and the density profile is much more accurate. This shows that it may indeed be useful to directly approximate the KP, and that simple local approximations can give a good average description. However, the exact $V_{T_s}(\mathbf{r};[\rho])$ must still be nonlocal, and detailed features of the density profile for atoms like shell structure cannot be reproduced by such a simple gradient correction. A truly nonlocal $V_{T_s}(\mathbf{r};[\rho])$ satisfying the two limiting forms of the exact KP and the exact LR function is desirable. Two new nonlocal KPs with these properties will be presented in Chapter 4.

3.6 LR-based Kinetic Energy Density Functionals

Recent nonlocal KEDFs applied to solids were based on satisfying LR theory. A general trial functional was written as

$$T_s[\rho] = T_{TF}[\rho] + T_W[\rho] \\ +C_F \int\int w_{\alpha,\beta}(\mathbf{r}-\mathbf{r}'; k_F(\mathbf{r},\mathbf{r}'))\rho^\alpha(\mathbf{r})\rho^\beta(\mathbf{r}')d\mathbf{r}d\mathbf{r}', \tag{3.22}$$

where α and β are positive parameters chosen by various arguments [14, 15, 22, 23, 26]. Here $k_F(\mathbf{r},\mathbf{r}')$, the scaling variable in $w_{\alpha,\beta}(\mathbf{r}-\mathbf{r}'; k_F(\mathbf{r},\mathbf{r}'))$, is the *two-body Fermi wave vector* (TBFWV), and approximations must be made to its form to have a well defined model. Once this is done, then the weight function $w_{\alpha,\beta}(\mathbf{r}-\mathbf{r}'; k_F(\mathbf{r},\mathbf{r}'))$ is uniquely determined by imposing LR in the homogeneous limit. However, there is no reason to believe that the exact $T_s[\rho]$ can be written in this form, and it is not known what errors are introduced by using this mathematical ansatz in nonlinear regimes.

Clearly, the TBFWV $k_F(\mathbf{r},\mathbf{r}')$ should reduce to the FWV k_F in the homogeneous limit when $\rho(\mathbf{r}) \to \rho_0$, and, at least for slowly varying density distributions, to the *local* FWV

$$k_F(\mathbf{r}) \equiv (3\pi^2\rho(\mathbf{r}))^{1/3}, \tag{3.23}$$

as $\mathbf{r}' \to \mathbf{r}$, so that

$$\lim_{\rho(\mathbf{r})\to\rho_0} k_F(\mathbf{r},\mathbf{r}') = k_F \tag{3.24}$$

and

$$\lim_{\mathbf{r}'\to\mathbf{r}} k_F(\mathbf{r},\mathbf{r}') = k_F(\mathbf{r}). \tag{3.25}$$

Further specifications for $k_F(\mathbf{r},\mathbf{r}')$ have to be made for general inhomogeneous systems. In the KEDFs proposed by Smargiassi and Madden (SM) [22] and by Perrot [23], the simplest choice $k_F(\mathbf{r},\mathbf{r}') = k_F$ in Eq. (3.24) is used. Since the mean density $\rho_0 = N/V$ of the system is required, their KEDFs can not be applied to isolated systems, such as atomic or molecular systems.

On different grounds, Wang and Teter (WT) argued that any choice of an average Fermi momentum will not work very well in general, and they proposed a somewhat complicated path-integral-like scheme to extend the WT KEDF (with $k_F(\mathbf{r},\mathbf{r}') = k_F$ for solids) to highly nonuniform systems, such as atoms [26]. Nevertheless, when applied to atoms, the nonlocal part of their proposed kinetic potential diverges as $r \to \infty$, while the correct asymptotic form should approach zero.

In the work of Wang, Govind, and Carter (WGC), $k_F(\mathbf{r},\mathbf{r}') = k_F$ was originally used for solids [14], and they later introduced a density dependence into the kernel with an approximate $k_F(\mathbf{r},\mathbf{r}')$ [15], as will be discussed below.

A different trial functional for the KEDF was proposed by Chacón, Alvarellos, and Tarazona (CAT) [19]

$$T_s[\rho] = T_W[\rho] - \frac{3}{5}T_{TF}[\rho] + \frac{8}{5}C_F \int \rho(\mathbf{r})\,[\bar{\rho}(\mathbf{r})]^{(2/3)} d\mathbf{r} \tag{3.26}$$

with $\bar{\rho}(\mathbf{r})$ being a weighted average of the density,

$$\bar{\rho}(\mathbf{r}) = \int w(\mathbf{r}-\mathbf{r}'; k_F(\mathbf{r},\mathbf{r}'))\rho(\mathbf{r}')d\mathbf{r}', \tag{3.27}$$

where $w(\mathbf{r}-\mathbf{r}'; k_F(\mathbf{r},\mathbf{r}'))$ is a normalized weight function determined by the LR requirement in the homogeneous limit. Again a further ansatz must be made for $k_F(\mathbf{r},\mathbf{r}')$. In the original CAT KEDF, $k_F(\mathbf{r},\mathbf{r}') = k_F(\mathbf{r})$ was adopted. This was

further generalized by García-González, Alvarellos, and Chacón (GAC) with an approximate $k_F(\mathbf{r}, \mathbf{r}')$, as will be discussed below [20, 21].

All these schemes require specification of $k_F(\mathbf{r}, \mathbf{r}')$. Both k_F and $k_F(\mathbf{r})$ have been widely used, due to their simplicity and computational efficiency. Fast Fourier transforms can then be performed for the nonlocal term in the KEDFs, and can achieve a fast computation of $O(M \ln M)$, where M is the integration grid size. Those KEDFs using $k_F(\mathbf{r}, \mathbf{r}') = k_F$ in the weight functions have simple and analytical forms for the resulting weight functions in Fourier space. However, the mean density ρ_0 of the system is needed as an input in these approaches. As a result, they can not be applied to isolated systems, such as atoms and molecules, where $\rho_0 = 0$.

Those KEDFs that use a local FWV $k_F(\mathbf{r})$ in the weight functions have been applied to atoms and metallic jellium surfaces. However, a first-order differential equation has to be solved numerically for their weight functions in Fourier space. Using a parameterization of the weight function can lead to an analytical form, but any parameterization of the weight function will not include the important singularity at $q = 1$ [20]. Using these approaches, only incipient shell structure for heavy closed-shell atoms can be obtained, probably due in part to the incomplete description of $k_F(\mathbf{r}, \mathbf{r}')$ but more basically because the external potential is far from the LR regime.

In general, if the density variations of the model system are significantly different from its average or local density, the TBFWV $k_F(\mathbf{r}, \mathbf{r}')$ could be quite different from k_F and $k_F(\mathbf{r})$. Taking account of the symmetry of $k_F(\mathbf{r}, \mathbf{r}')$ in $\mathbf{r}$ and $\mathbf{r}'$, a more general choice for the TBFWV has been proposed in recent KEDFs, [14, 15, 20, 21]

of the form

$$k_F^\gamma(\mathbf{r},\mathbf{r}') = \left(\frac{k_F^\gamma(\mathbf{r}) + k_F^\gamma(\mathbf{r}')}{2}\right)^{1/\gamma}, \tag{3.28}$$

where γ is a parameter. Clearly, $k_F^\gamma(\mathbf{r},\mathbf{r}')$ satisfies Eq. (3.24) and (3.25) for any γ but there is no fundamental justification for this particular functional form.

GAC empirically found that $|\gamma|$ should be less than unity for atoms, and $\gamma = -\frac{1}{2}$ gives the best atomic energy for light atoms using the GAC KEDF [20]. Also, the GAC KEDF shows a clearer shell structure of atoms than that predicted by their previously proposed CAT KEDF, with $k_F(\mathbf{r},\mathbf{r}') = k_F(\mathbf{r})$ [19]. However, the CAT KEDF has convergence problems in extended systems, and the GAC KEDF gives an unphysical density profile for metallic surfaces. Thus a different choice of $\gamma = \frac{1}{2}$ has to be adopted for metallic surfaces [21]. With $\gamma = \frac{1}{2}$, the GAC KEDF can be used for both atoms and metallic surfaces, but the atomic shell structure, and atomic energy become less accurate than that with $\gamma = -\frac{1}{2}$. Most likely, different choices of γ will have to be adopted for different systems, such as molecular clusters and solids, although calculations on these systems have not been done due to the expensive $O(M^2)$ numerical scaling of GAC KEDF.

With the same form of $k_F^\gamma(\mathbf{r},\mathbf{r}')$, Wang, Govind, and Carter (WGC) [15] empirically found that $\gamma = 2.7$ gives very good results for bulk aluminum with their proposed WGC KEDF. Because the use of $k_F^\gamma(\mathbf{r},\mathbf{r}')$ results in an expensive quadratic $O(M^2)$ scaling with system size, WGC use a truncated Taylor series expansion to describe the density dependence in their weight function to reach essentially linear scaling $O(M \ln M)$. Nevertheless, a reference uniform density ρ_* is needed in that

scheme. For bulk solids, the natural choice for ρ_* is the bulk density ρ_0. For a system with large density variations, like atoms and molecules, this scheme suffers due to the lack of a proper choice of ρ_*. In a recent paper [18], they found that $\gamma = 2.7$ is not the optimal choice for silicon, and they further argued that there is no universal γ for various materials.

In summary, recent advance in OF-DFT have shown that incorporating the correct limiting forms of the exact KEDF, and the exact LR in the homogeneous limit into a trial KEDF can generate more accurate nonlocal KEDFs that can give good results for extended metallic systems and give some indications of shell structure for atoms. However, there are also notable failures and inconsistencies. We believe there are two related conditions that should hold before such LR-based KEDFs can be generally applied with confidence. One is that the model potential should be weak enough to be within the LR regime to the extent possible and the other is that the electron density in the model system should be slowly-varying enough that highly nonlocal approximations to $k_F(\mathbf{r}, \mathbf{r}')$ are not needed.

Regarding to the past failures of using $k_F(\mathbf{r}, \mathbf{r}') = k_F^{\gamma}(\mathbf{r}, \mathbf{r}')$ in different systems, we believe that it is not likely that one can find a generally applicable $k_F(\mathbf{r}, \mathbf{r}')$ for the systems with large density variations, because of further unknown errors in the postulated functional forms of the approximate KEDFs away from the linear response regime. Computationally, the use of a general $k_F(\mathbf{r}, \mathbf{r}')$ in KEDFs leads to an expensive quadratic scaling $O(M^2)$, and a second-order differential equation for the weight functions in Fourier space.

In our proposed nonlocal LR-based KPs discussed in the next section, it is nat-

ural to use the simple local approximation $k_F(\mathbf{r})$ for the FWV. Clearly, this choice satisfies the Eq. (3.24) and (3.25), and fast Fourier transforms can be performed to reach essentially linear scaling with the system size. We argue that such a local approximation is more likely to be useful when used directly in the KP rather than the KEDF. Moreover, to describe atom-based systems such as atoms, molecules and solids, where the full density variations are large and the model potentials are divergent at each nucleus, we show in Chapter 4 how to construct a weak and slowly-varying local pseudopotential that generates a slowly varying valence density component more suitable for OF approximations. We believe that both steps, exploiting the simpler form of the KP, and using the OF theory only for the valence component, will be needed for quantitative work in many cases.

Chapter 4

Kinetic Potentials and Pseudopotentials

4.1 Construction of Nonlocal Kinetic Potentials

It has been noticed that the exact $T_s[\rho]$ in one spatial dimension satisfies the following inequality [2]:

$$T_W[\rho] \leq T_s[\rho] \leq T_W[\rho] + T_{TF}[\rho] \tag{4.1}$$

For densities deviating sightly from uniformity, Eq. (4.1) was found to be correct even in three dimensions [25]. In three dimensions, whether the upper bound generally holds remains an open question, though the lower bound always holds [2, 25]. Since the $T_W[\rho]$ appears in both the lower and upper bounds of $T_s[\rho]$, it seems plausible that one should keep the full $T_W[\rho]$ in constructing an approximate $T_s[\rho]$ and modify the $T_{TF}[\rho]$ term. This suggests that one should focus on improving the WλTF KEDFs.

As argued before, it may be more profitable to take advantage of known limiting forms of the kinetic potential, rather than the KEDF, and develop approximations for the simpler $V_{T_s}(\mathbf{r};[\rho])$ directly. Nonlocal effects may be less problematic and we can rely on known results in the linear response regime when the density variations are not too large.

As discussed in Chapter 3, the following linear combinations of the TF KP

and the W KP in Eqs. (3.12) and (3.13) can reproduce exact results to second order for very small and very large wavevector perturbations respectively:

$$V_{T_s}(\mathbf{r};[\rho]) \approx \begin{cases} V_{TF}(\mathbf{r};[\rho]) + \frac{1}{9}V_W(\mathbf{r};[\rho]) & q \ll 1 \\ V_W(\mathbf{r};[\rho]) - \frac{3}{5}V_{TF}(\mathbf{r};[\rho]) & q \gg 1 \end{cases} \tag{4.2}$$

Since $V_{TF}(\mathbf{r};[\rho])$ and $V_W(\mathbf{r};[\rho])$ are the only components, up to second order, of the two limiting forms of the exact KP, instead of combining them with a fixed parameter λ, it seems natural to allow a wavevector dependence in $\lambda = \lambda(q)$ to connect the limiting forms. Moreover the $\lambda(q)$ can be chosen in a very simple way so that the exact LR function can be reproduced for a uniform system with density ρ_0. In this way the LR function *bridges* the exact limits at large and small wavevectors, and if the theory is applied to perturbations in the linear response regime for intermediate wavevectors we can expect very accurate results. Here, we derive such generalized KPs based on the KPs for the WλTF KPs.

4.2 HQ Kinetic Potential

Based on Eq. (4.2) and in analogy to the WλTF model in Eq. (3.10) we first look for a kinetic potential of the form

$$V^0_{HQ}(\mathbf{k}) = V_W(\mathbf{k}) + \lambda_{HQ}(q)\ V_{TF}(\mathbf{k}), \tag{4.3}$$

where

$$q = k/2k_F \tag{4.4}$$

is a dimensionless wavevector normalized by the FWV k_F in Eq. (3.5) of a uniform reference system with density ρ_0. The superscript 0 in V^0_{HQ} indicates use of this

uniform reference system. For a small perturbation, we can linearize the $V^0_{HQ}(\mathbf{k})$ in Eq. (4.3). Requiring that it satisfy LR exactly then determines $\lambda_{HQ}(q)$ as

$$\lambda_{HQ}(q) = F_L(q) - 3q^2. \tag{4.5}$$

The two limiting forms of the $\lambda_{HQ}(q)$ are

$$\lambda_{HQ}(q) = \begin{cases} 1 + O(q^2) & q \ll 1 \\ -\frac{3}{5} + O(q^{-2}) & q \gg 1 \end{cases} \tag{4.6}$$

Inserting Eq. (4.6) into Eq. (4.3), we obtain the two limiting forms of the proposed $V_{HQ}(\mathbf{k})$:

$$V^0_{HQ}(\mathbf{k}) = \begin{cases} V_{TF}(\mathbf{k}) + \cdots & q \ll 1 \\ V_W(\mathbf{k}) - \frac{3}{5} V_{TF}(\mathbf{k}) + \cdots & q \gg 1 \end{cases} \tag{4.7}$$

where $\cdots$ indicates that the following terms are not exact higher order terms.

Since this model reduces to the correct high-q limit in Eq. (4.2) up to the second order, and to the correct low-q only to the leading order, we denote this kinetic potential as the HQ KP.

Since $V_{TF}(\mathbf{r};[\rho])$ and $V_W(\mathbf{r};[\rho])$ are the leading components of the two limiting forms of the exact KP, it is instructive to keep these two terms in full, and treat the remaining term as their correction. After subtracting $V_{TF}(\mathbf{k})$, Eq. (4.3) can be rewritten as

$$\begin{aligned} V^0_{HQ}(\mathbf{k}) &= V_{TF}(\mathbf{k}) + V_W(\mathbf{k}) + (\lambda_{HQ}(q) - 1)\, V_{TF}(\mathbf{k}) \\ &= V_{TF}(\mathbf{k}) + V_W(\mathbf{k}) + \hat{f}(q)\, V_{TF}(\mathbf{k}), \end{aligned} \tag{4.8}$$

Figure 4.1: Weight functions $\hat{f}(q)$ for the HQ KP.

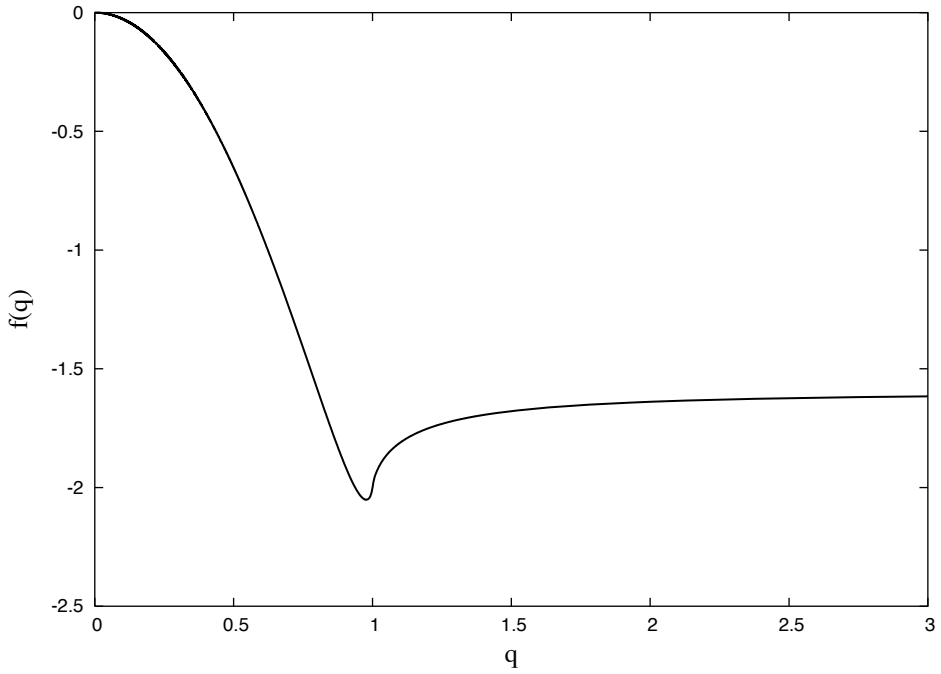

where the weight function $\hat{f}(q)$ is

$$\hat{f}(q) = F_L(q) - 3q^2 - 1. \tag{4.9}$$

After inverse Fourier transform of Eq. (4.8) to real space, this gives

$$\begin{aligned} V^0_{HQ}(\mathbf{r};[\rho],k_F) &= V_{TF}(\mathbf{r};[\rho]) + V_W(\mathbf{r};[\rho]) \\ &+ \int f(|\mathbf{r}-\mathbf{r}'|;k_F)\ V_{TF}(\mathbf{r}';[\rho])d\mathbf{r}'. \end{aligned} \tag{4.10}$$

This expression is directly useful for metallic systems where a reasonable ρ_0 can be defined. For systems such as atoms and molecules where the density vanishes far from the nuclei, it is natural to replace k_F in Eq. (4.10) by the *local* Fermi wavevector in Eq. (3.23) .

This yields the general form of our proposed HQ kinetic potential as

$$V_{HQ}(\mathbf{r};[\rho],k_F(\mathbf{r})) = V_{TF}(\mathbf{r};[\rho]) + V_W(\mathbf{r};[\rho]) \\ +\tfrac{5}{3}C_F\int f(|\mathbf{r}-\mathbf{r}'|;k_F(\mathbf{r}))\ \rho^{2/3}(\mathbf{r}')d\mathbf{r}'. \tag{4.11}$$

Note that the last term in Eq. (4.11) is most easily computed in Fourier space as

$$\frac{5C_F}{3(2\pi)^3}\int \hat{f}(k/2k_F(\mathbf{r}))\rho^{2/3}(\mathbf{k})e^{-i\mathbf{k}\cdot\mathbf{r}}d\mathbf{k}, \tag{4.12}$$

As can been seen in Eq. (4.9), the weight function $\hat{f}(k/2k_F(\mathbf{r}))$ is determined analytically. Unlike the KEDF approach, no first-order differential equation (with $\xi_F(\mathbf{r},\mathbf{r}') = k_F(\mathbf{r})$) is needed to solve for the weight function in Fourier space.

4.3 LQ Kinetic Potential

We use the generalized WλTF KPs to suggest the form of the HQ KP. One might hope that a more systematic search using generalized forms of this kind could yield even better results. We considered one such generalization of the nonlocal term in the HQ KP that allows for the introduction of a parameter α, and that interpolates between the TF and W KPs using linear response theory of uniform systems:

$$V_\alpha(\mathbf{r};[\rho],k_F(\mathbf{r})) = V_{TF}(\mathbf{r};[\rho]) + V_W(\mathbf{r};[\rho]) \\ +\tfrac{2}{3\alpha}V_\alpha^{nloc}(\mathbf{r};[\rho],k_F(\mathbf{r})) \tag{4.13}$$

where the $V_\alpha^{nloc}(\mathbf{r};[\rho],k_F(\mathbf{r}))$ is defined as

$$V_\alpha^{nloc}(\mathbf{r};[\rho],k_F(\mathbf{r})) = \frac{5}{3}C_F[\rho(\mathbf{r})]^{(2/3-\alpha)}\int f(|\mathbf{r}-\mathbf{r}'|;k_F(\mathbf{r}))\ \rho^\alpha(\mathbf{r}')d\mathbf{r}' \tag{4.14}$$

The two limiting forms of the $\hat{f}(q)$ are

$$\hat{f}(q) = \begin{cases} -\frac{8}{3}q^2 + O(q^4) & q \ll 1 \\ \\ -\frac{8}{5} + O(q^{-2}) & q \gg 1 \end{cases}, \tag{4.15}$$

and the corresponding two limits of $V_\alpha^{nloc}(\mathbf{r};[\rho],k_F(\mathbf{r}))$ are

$$V_\alpha^{nloc}(\mathbf{r};[\rho],k_F(\mathbf{r})) \approx \begin{cases} \nabla^2\rho^\alpha/3\rho^\alpha & q \ll 1 \\ \\ -\frac{8}{5}V_{TF}(\mathbf{r};[\rho]) & q \gg 1 \end{cases} \tag{4.16}$$

For $\alpha = 2/3$, this reduces to the HQ KP. For $\alpha = 1/2$, this KP satisfies the correct low-q limit in Eq. (4.2) up to the second order, and the high-q limit only to leading order, and we denote this choice of kinetic potential as the LQ KP.

$$\begin{aligned} V_{LQ}(\mathbf{r};[\rho],k_F(\mathbf{r})) &= V_{TF}(\mathbf{r};[\rho]) + V_W(\mathbf{r};[\rho]) \\ &+\tfrac{20}{9}C_F\rho^{1/6}(\mathbf{r})\int f(|\mathbf{r}-\mathbf{r}'|;k_F(\mathbf{r}))\ \rho^{1/2}(\mathbf{r}')d\mathbf{r}' \end{aligned} \tag{4.17}$$

Among these one-parameter generalized KPs in Eq. (4.13), there is no single value of α that can generate a KP that satisfies both of the correct LQ and HQ limits up to second order. To achieve this, one can try a linear combination of these types of nonlocal KP with two different α's. The detailed description of how to construct the LHQ KPs is in Appendix A.

4.4 Linear Scaling Method

Due to the $k_F(\mathbf{r})$ term in the nonlocal term of Eq. (4.14) , all these models scale quadratically. In order to achieve linear scaling, we apply Taylor series expansions to the weight functional $f(|\mathbf{r}-\mathbf{r}'|; k_F(\mathbf{r}))$ with respect to a reference density ρ_*. This approach is similar to that proposed by Wang *et al* [15], where $k_F^{\gamma}(\mathbf{r}, \mathbf{r}')$ (see Eq. (3.28)) is in their weight kernel.

$$\begin{aligned} f(|\mathbf{r}-\mathbf{r}'|; k_F(\mathbf{r})) = f(|\mathbf{r}-\mathbf{r}'|; k_F^*) + f^{(1)}(|\mathbf{r}-\mathbf{r}'|; k_F^*)(\rho(\mathbf{r})-\rho_*) \\ + f^{(2)}(|\mathbf{r}-\mathbf{r}'|; k_F^*)\frac{(\rho(\mathbf{r})-\rho_*)^2}{2!} + f^{(3)}(|\mathbf{r}-\mathbf{r}'|; k_F^*)\frac{(\rho(\mathbf{r})-\rho_*)^3}{3!} + \cdots . \end{aligned} \tag{4.18}$$

where $k_F^* \equiv (3\pi^2\rho_*)^{1/3}$, and $f^{(n)}(|\mathbf{r}-\mathbf{r}'|; k_F^*) = \frac{\partial^n f(|\mathbf{r}-\mathbf{r}'|; k_F(\mathbf{r}))}{\partial \rho^n(\mathbf{r})} \mid_{\rho_*}$ is the nth order derivative of $f(|\mathbf{r}-\mathbf{r}'|; k_F(\mathbf{r}))$ with respect to $\rho(\mathbf{r})$, and is evaluated at ρ_*. Their functional forms, up to the third order, in reciprocal space are

$$\hat{f}^{(1)}(q_*) = -\frac{q_*}{3\rho_*}\hat{f}'(q_*) \tag{4.19}$$

$$\hat{f}^{(2)}(q_*) = \frac{q_*^2\hat{f}''(q_*) + 4q_*\hat{f}'(q_*)}{(3\rho_*)^2} \tag{4.20}$$

$$\hat{f}^{(3)}(q_*) = -\frac{q_*^3\hat{f}'''(q_*) + 12q_*^2\hat{f}''(q_*) + 28q_*\hat{f}'(q_*)}{(3\rho_*)^3} \tag{4.21}$$

where $q_* = \frac{k}{2k_F^*}$, and $\hat{f}'(q_*)$, $\hat{f}''(q_*)$, and $\hat{f}'''(q_*)$ are the first, the second and the third derivative of $\hat{f}(q)$ with respect to q_*. Since the analytical form of $\hat{f}(q)$ is available in Eq. (4.9) , all the kernel needed in the Taylor series expansion $\hat{f}^{(n)}(q)$, can be obtained analytically.

By carrying out the Taylor series expansion to the nth order in Eq. (4.18), and inserting it to Eq. (4.14), one can then take out the $(\rho(\mathbf{r}) - \rho_*)^m$ of the mth term from its integral (where m is a nonnegative integer, and $m \leq n$), and the remaining integral becomes:

$$\int f^{(m)}(|\mathbf{r} - \mathbf{r}'|; k_F^*)\ \rho^\alpha(\mathbf{r}')d\mathbf{r}' \tag{4.22}$$

The integral in Eq. (4.22) can be easily evaluated by a simple FFT. Therefore, to compute the nonlocal term in Eq. (4.14), using this scheme, one needs to evaluate a total of $n+2$ FFTs, including the FFT of ρ^α. Since all of the terms can be computed by FFT, this scheme essentially scales linearly $O(M \ln M)$ with system size.

For extended systems, where $\rho(\mathbf{r})$ is not significantly different from the uniform density ρ_0, the natural choice of ρ_* is, of course, ρ_0. In this dissertation, we choose $\rho_* = \rho_0$, and carry out our calculations up to the first order. For isolated systems, or the extended systems with large density variations over space, this method may experience convergence problems, like the WGC KEDF [15, 16, 18].

4.5 Kinetic Energy of the LQ and HQ KPs

4.5.1 Isolated Systems

As discussed in Chapter 2, unlike the KEDF approaches, we directly construct the KPs, and compute the kinetic energy via various pathways. If the approximate $V_{T_s}(\mathbf{r}; [\rho])$ used in the integration is accurate, then all pathways would give very similar results for $T_s[\rho]$.

For isolated systems, the Herring's pathway (see Eq. (2.2)) is the most appealing one, since it satisfies the viral theorem, and it is computationally efficient. The kinetic energy of the LQ ($\alpha = 1/2$) and HQ ($\alpha = 2/3$) KPs in Eq. (4.13) using this pathway is

$$\begin{aligned} T_\alpha[\rho] &= T_{TF}[\rho] + T_W[\rho] \\ &\quad + \frac{2}{3\alpha} \int d\mathbf{r} \int d\mathbf{r}' V_\alpha^{nloc}(\mathbf{r}; [\rho], k_F(\mathbf{r})) \\ &\quad \times \bigtriangledown \cdot (\mathbf{r}\rho(\mathbf{r})) \end{aligned} \tag{4.23}$$

It should be noted that Eq. (4.23) is used for computing the numerical value of the kinetic energy of the LQ or the HQ model, and should not be regarded as a KEDF for generating the KP.

4.5.2 Extended Systems

For extended systems, Herring's pathway does not hold. Here, we adopt the linear density pathway in Eq. (2.4), due to its computational efficiency (see Chapter 2).

Using this pathway, the kinetic energy of the LQ and HQ KPs is

$$\begin{aligned} T_\alpha = T_{\lambda=0} + \textstyle\int_0^1 d\lambda \int d\mathbf{r} [\rho(\mathbf{r}) - \rho_0] \{ V_{TF}(\mathbf{r}; [\rho_\lambda]) + V_W(\mathbf{r}; [\rho_\lambda]) + \\ + \tfrac{2}{3\alpha} V_\alpha^{nloc}(\mathbf{r}; [\rho_\lambda], k_F^\lambda(\mathbf{r})) \} \end{aligned} \tag{4.24}$$

$$k_F^\lambda(\mathbf{r}) \equiv (3\pi^2 \rho_\lambda(\mathbf{r}))^{1/3}. \tag{4.25}$$

As discussed in Chapter 2, if one choose the reference system as the uniform system, the kinetic energy of the reference system is simply the TF KEDF with $\rho(\mathbf{r}) = \rho_0$ ($T_{\lambda=0} = T_{TF}[\rho] \mid_{\rho(\mathbf{r})=\rho_0}$). Since the $V_{TF}(\mathbf{r};[\rho_\lambda])$ and $V_W(\mathbf{r};[\rho_\lambda])$ in Eq. (4.24) are from the functional differentials of the $T_{TF}[\rho]$ and $T_W[\rho]$ respectively, these terms can be integrated exactly and lead to the TF and W KEDFs. Eq. (4.24) then becomes

$$\begin{aligned} T_\alpha[\rho] &= T_{TF}[\rho] + T_W[\rho] + \\ &\quad + \int_0^1 d\lambda \int d\mathbf{r}[\rho(\mathbf{r}) - \rho_0] \ \tfrac{2}{3\alpha} V_\alpha^{nloc}(\mathbf{r};[\rho_\lambda], k_F^\lambda(\mathbf{r}))\} \end{aligned} \tag{4.26}$$

where $T_{\lambda=0} = T_{TF}[\rho] \mid_{\rho(\mathbf{r})=\rho_0}$ term is absorbed in the $T_{TF}[\rho]$ term.

Similarly, for the linear scaling method described in the previous section, the kinetic energy of the LQ, and HQ KPs from Eqs. (4.13, 4.14, and 4.18), is computed as

$$\begin{aligned} T_\alpha[\rho] \;=\; & T_{TF}[\rho] + T_W[\rho] + \int_0^1 d\lambda \int d\mathbf{r}[\rho(\mathbf{r}) - \rho_0] \ \frac{10}{9\alpha} C_F[\rho_\lambda(\mathbf{r})]^{(2/3-\alpha)} \\ & \int d\mathbf{r}'\{f(|\mathbf{r}-\mathbf{r}'|;k_F^*) + f^{(1)}(|\mathbf{r}-\mathbf{r}'|;k_F^*)(\rho_\lambda(\mathbf{r}) - \rho_*) \\ & + f^{(2)}(|\mathbf{r}-\mathbf{r}'|;k_F^*)\frac{(\rho_\lambda(\mathbf{r}) - \rho_*)^2}{2!} + \cdots\} \ [\rho_\lambda(\mathbf{r}')]^\alpha \end{aligned} \tag{4.27}$$

4.6 Generation of *Ab Initio* Local Pseudopotentials

Since our nonlocal KPs are based on the LR theory of uniform systems, one would not expect the LR-based OF-DFT to work well when the model potentials are well beyond the LR regime. To enhance the performance of the LR-based OF-DFT,

a weak and slowly varying potential is certainly desirable.

In most chemical applications, the core electrons remain inactive and strongly bonded to the nuclei, and only the valence density responds to changes in the local environment. The strong nuclear potentials experienced by all electrons can then be replaced by a much weaker pseudopotential acting only on the valence electrons. This simplifying feature has been used to lessen the cost of many orbital-based calculations, since the valence orbitals are usually slowly-varying and fewer basis functions are needed to approach the model limit. For the recently proposed non-local LR-based OF-DFT, the use of local pseudopotentials not only can reduce the computational cost, but also can improve the accuracy because the resulting pseudopotential is weaker, and thus more nearly in the LR regime, where the theory is designed to be accurate.

Because of the one-to-one mapping between the effective one-body potential acting on a system of N electrons and the electron density in the ground-state configuration, it is possible to obtain a unique local one-body potential that generates a given density by using a KS-like orbital-based method in an inverse way [46]. Let us decompose the total electron density $\rho(\mathbf{r})$ of a given atom into a "core density" $\rho_c(\mathbf{r})$, which is supposed not to vary significantly in other molecular or solid state environments, and the "valence density" $\rho_v(\mathbf{r})$ where

$$\rho(\mathbf{r}) = \rho_v(\mathbf{r}) + \rho_c(\mathbf{r}). \tag{4.28}$$

Because DFT requires only the total electron density, we can take a more general view of what is meant by the core and valence components than is used in most

orbital-based methods. Following AILPS methods [17, 47], for a given $\rho_v(\mathbf{r})$, the inverse-KS equations are solved to get the corresponding one-body screened potential $V_{scr}(\mathbf{r})$. The desired *ab initio* local pseudopotential $V_{ps}(\mathbf{r})$ (AILPS) is then obtained by subtracting the Hartree potential and the exchange-correlation potential:

$$V_{ps}(\mathbf{r}) = V_{scr}(\mathbf{r}) - V_H(\mathbf{r};[\rho_v]) - V_{xc}(\mathbf{r};[\rho_v]), \tag{4.29}$$

This relatively expensive procedure to determine $V_{ps}(\mathbf{r})$ requires the use of orbitals. However it needs to be done only once for each atom, and the resulting $V_{ps}(\mathbf{r})$ can be used for other problems if the atomic core density remains essentially constant.

In order to use pseudopotential methods with OF-DFT, a target valence density must be chosen. In most applications to date, a different nonlocal pseudopotential calculation is carried out to generate such a target density. This is not only computationally expensive, but also inflexible in specifying a desirable form of $\rho_v(r)$ for OF-DFT. For the LR-based OF-DFT we consider, a smooth valence density with small variations from its average in the core region is the most important requirement, both for using the local FWV $k_F(\mathbf{r})$ and for generating a model system closer to the linear response regime.

Here we directly construct such a smooth valence density for the $N_v = N - N_c$ valence electrons, with N_c a given number of core electrons, here chosen to be the number of electrons in the noble gas configuration. We find most results do not depend on the details of our fitting procedure. Our proposed valence density $\tilde{\rho}_v(r)$ for atoms equals the full KS density $\rho_{KS}(r)$ outside a core radius r_c, and has the

following smooth form inside r_c:

$$\tilde{\rho}_v(r) = \begin{cases} t\rho_{KS}(r_c) + a_0 r^q \exp[-r^p(a_1 + a_2 r^2)] & r \le r_c \\ \\ \rho_{KS}(r) & r > r_c \end{cases} \tag{4.30}$$

Here p and q are given positive numbers, which we generally take as even integers for concreteness. To avoid producing a cusp in $\tilde{\rho}_v(r = 0)$, we choose $p \ge 2$ and $q \ge 2$. The larger they are, the more rapidly varying is the valence density in the core region (see Fig. (4.2)), and then the larger and the more rapidly varying is the local pseudopotential $V_{ps}(r)$ (see Fig. (4.3)). For applications in different environments, such as molecules or crystals, the core size r_c has to be small to maintain transferability of the atomic core density. For this reason, we force $\tilde{\rho}_v(r = 0)$ to be small by taking a small t. Without this term ($t = 0$), the vanishing of the valence density near the nucleus will require a very repulsive V_{ps}, which is certainly undesirable for the LR-based OF-DFT. However, we found that if t is too large, there will exist a long oscillatory tail outside the core in the corresponding $V_{ps}(r)$. This is an undesirable feature, as will be discussed below. The above two points constrain the value of t. In this dissertation, we choose $t = 0.1$ for all the AILPS of pseudoatoms.

The four parameters a_0, a_1, a_2, and r_c are determined by requiring continuity of the function $\tilde{\rho}_v(r)$ and its first two derivatives at $r = r_c$, and by satisfying the normalization condition:

$$N - N_c = 4\pi \int \tilde{\rho}_v(r) r^2 dr. \tag{4.31}$$

In contract to the traditional pseudopotential methods, N_c could in principle be

fractional in this scheme and not necessarily equal to number of electrons in the noble-gas configurations. This feature might provide additional flexibility in choosing a suitable r_c that could maximize transferability of the cores in different systems. However we have not investigated this possibility, and use the standard noble gas cores in what follows.

To construct our local pseudopotential $V_{ps}(r)$ for atoms, we first solve the KS equations for an atom with the full Coulomb potential. With the KS density $\rho_{KS}(r)$ thus determined, and a plausible guess for N_c, which here we take to be the number of core electrons in the closed-shell configuration. Note by this construction that the associated core density smoothly approaches zero as $O(\mid r - r_c \mid^3)$ as $r \to r_c$. Indeed as shown below, with an acceptable N_c, essentially the same density profiles are predicted by the LQ and HQ models for a very wide range of p, q, and t. This would be expected if most features of the resulting model potentials are within the different regimes accurately described by the OF KP.

After generating the parameterized valence density $\tilde{\rho}_v(r)$, a set of inverse-KS equations are then solved to obtain the corresponding one-body screened potential $V_{scr}(r)$. After removing the contributions from the Hartree and exchange-correlation potentials, the AILPS $V_{ps}(r)$ is obtained (see Eq. (4.29)) and the reference system for an atom is thus constructed.

We found that the $rV_{ps}(r)$ constructed this way for group III to group VIII elements deviates from $-Z$ outside the core by a small and long range oscillation (see Fig. (4.4)). For the $2s^2 2p^x$ atoms, the maximum amplitude of the tails is about 0.18. For the $3s^2 3p^x$ atoms, it ranges from 0.003 for Al to 0.037 for Ar. Similar

Figure 4.2: The smooth valence density $\tilde{\rho}_v(r)$ from Eq. (4.30), with three different parameters (with $t = 0.1$) for the Si pseudoatom.

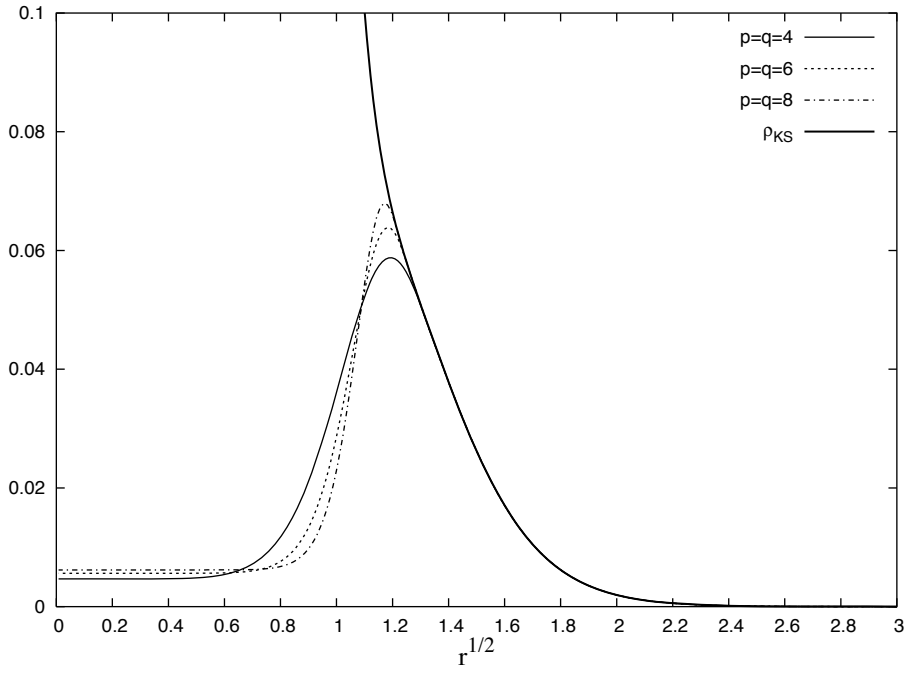

oscillatory tails were observed by Wang and Stott [47]. Physically, this oscillation is due to inability of representing both s and p orbitals of the corresponding nonlocal pseudopotentials by a simple local pseudopotential. We found that the existence of this long oscillatory tail in the AILPS of each atom does not significantly affect the density profile of the atom, because its magnitude is so small. However, since there should be no long range oscillatory tails in cores transferable from atoms to solids [81], modification of the AILPS $V_{ps}(r)$ is necessary for solid-state applications. Following Wang and Stott's approach, the AILPS $V_{ps}(r)$ is modified by truncating the tail at a point where $rV_{ps}(r) = -Z$. As shown in Fig. (4.4), the truncation can be made at two points, and truncation at larger r is made for all the cases here.

To apply the model to other chemical environments, such molecules and solids,

Table 4.1: Parameters used in Eq.(4.30) for the reference systems. Here, $p = q = 6$, and $t = 0.1$ are used for all the pseudoatoms. The $V_{ps}(r)$ generated by using this parameterized $\tilde{\rho}_v(r)$ is then used to construct a reference system.

	N	N_c	a_0	a_1	a_2	r_c	$t\rho_{KS}(r_c)$
Li	3	2	2.983×10^{-4}	0.05260	-6.560×10^{-3}	2.135	3.658×10^{-4}
Be	4	2	0.02655	0.7078	-0.2130	1.370	2.543×10^{-3}
B	5	2	0.8032	5.855	-3.531	0.9714	9.006×10^{-3}
C	6	2	11.53	30.17	-31.20	0.7429	0.02442
N	7	2	98.80	112.8	-180.2	0.5978	0.05509
O	8	2	592.7	338.9	-779.8	0.4981	0.1091
F	9	2	2750	871.4	-2744	0.4256	0.1961
Ne	10	2	1.052×10^4	1993	-8267	0.3707	0.3279
Na	11	10	5.234×10^{-5}	9.840×10^{-3}	-6.610×10^{-4}	2.904	2.700×10^{-4}
Mg	12	10	9.805×10^{-4}	0.04445	-5.002×10^{-3}	2.233	1.203×10^{-3}
Al	13	10	6.164×10^{-3}	0.1273	-0.02056	1.861	2.774×10^{-3}
Si	14	10	0.02942	0.3119	-0.06861	1.593	5.621×10^{-3}
P	15	10	0.1149	0.6864	-0.1979	1.390	0.01027
S	16	10	0.3841	1.390	-0.5100	1.231	0.01734
Cl	17	10	1.133	2.632	-1.201	1.103	0.02750
Ar	18	10	3.018	4.714	-2.624	0.9985	0.04154

Figure 4.3: The AILPS $V_{ps}(r)$ generated by the three different parameterized valence density $\tilde{\rho}_v(r)$ (see Fig. (4.2)).

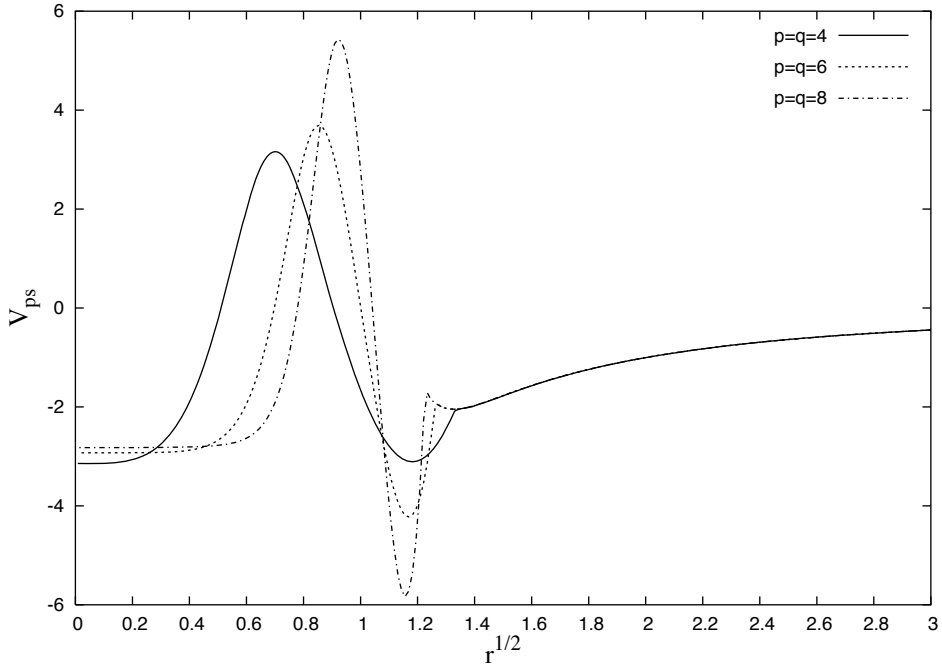

Figure 4.4: The $rV_{ps}(r)$ for $p = q = 6$, and $t = 0.1$ (see Fig. (4.3)). The two points, where $rV_{ps}(r) = -4$, are $r_1 = 2.336$ and $r_2 = 4.576$.

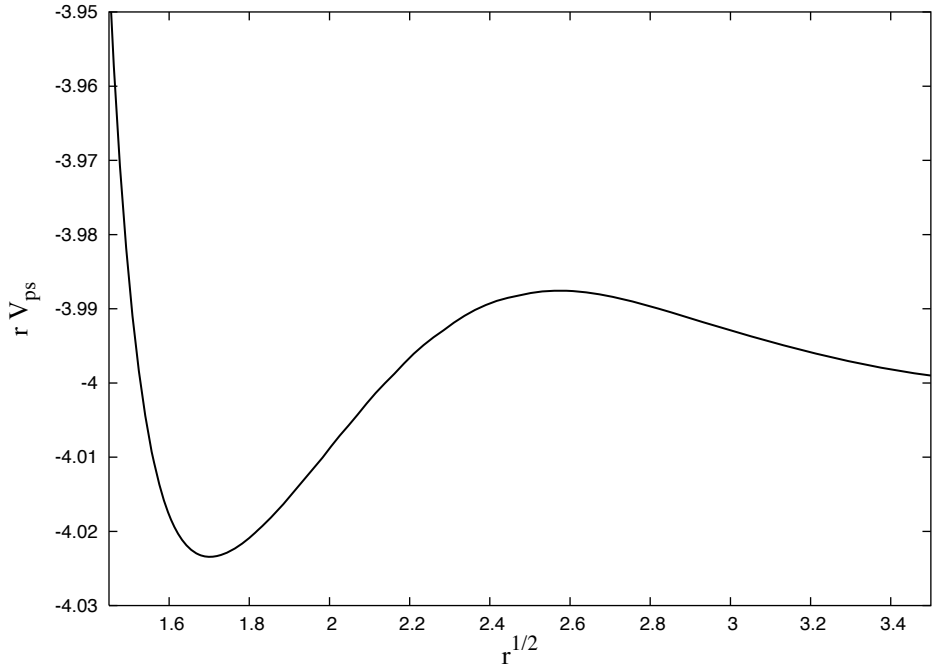

the predetermined AILPS $V_{ps}(\mathbf{r})$ centered at each nucleus are regarded as input data, and the valence densities for other systems are calculated by OF-DFT. Results can be checked by using the full KS-DFT. For example, for molecules and solids, the external potential $V_{ext}(\mathbf{r})$ is a linear combination of the local atomic pseudopotentials centered at each ion position $\mathbf{R}_I$:

$$V_{ext}(\mathbf{r}) = \sum_I V_{ps}(\mathbf{r} - \mathbf{R}_I) \tag{4.32}$$

Interaction between the core and valence electrons is described by $V_{ps}(\mathbf{r})$. The Euler equation for $\rho_v(\mathbf{r})$ is

$$\mu = V_{T_s}(\mathbf{r}; [\rho_v]) + V_H(\mathbf{r}; [\rho_v]) + V_{xc}(\mathbf{r}; [\rho_v]) + V_{ext}(\mathbf{r}), \tag{4.33}$$

where μ is the chemical potential (associated with the normalization condition of the valence electrons), and the total energy of valence electrons is

$$E_v[\rho_v] = T_s[\rho_v] + E_H[\rho_v] + E_{xc}[\rho_v] + \int \rho_v(\mathbf{r}) V_{ext}(\mathbf{r}) d\mathbf{r} \tag{4.34}$$

For the proposed LQ, HQ, and LHQ KPs, $T_s[\rho_v]$ in Eq. (4.34) is given from Eq. (2.2) with $\rho(\mathbf{r})$ replaced by $\rho_v(\mathbf{r})$.

In summary, we propose a simple and systematic way to generate a low and smooth valence density component consistent with a weak and slowly-varying AILPS. The time-consuming process of using KS-DFT inversely to determine the AILPS is only done once for each atom, and the resulting AILPS and core electron densities are then used as inputs in different chemical environments, such as molecules and solids. Since this approach can generate a low and slowly varying valence density inside the core, this also justifies the use of the local FWV in Eqs.

(3.23) and (4.11). Moreover, the resulting pseudopotential is relatively small and slowly varying, which justifies the use of the LR-based OF-KPs, such as LQ and HQ models.

Chapter 5

Applications of OF-DFT

5.1 Introduction

To understand the performance of the proposed OF models, we applied our LQ, HQ, and LHQ KPs to various systems, such as atoms, molecules, and solids, and compared the results to other KEDFs, KS-DFT, and experiment. Throughout this dissertation, we specify $\alpha_1 = 1/4$ in the LHQ KP (see Appendix A). The local density approximation (LDA) [68, 69, 70] for the exchange-correlation functional is used for all the models discussed here, unless noted otherwise.

For atoms, we performed both all-electron calculations using the full Coulomb potential, where we do not expect to find quantitative results in general, and *ab initio* local pseudopotential (AILPS) calculations using the valence density only. Our results are compared with the KS-DFT, and the TFλW models. For molecules, we performed the AILPS calculations, and compare our results of several diatomic molecules to the TFW model, the full KS-DFT, and experiment. For solids, we compare our results for bulk aluminum, and silicon, with other LR-based KEDFs, using the same local pseudopotentials as the previous workers. Calculations using our new AILPS for these systems are currently in progress.

5.2 Atoms

5.2.1 All-electron calculation

We define the *Pauli kinetic potential* $V^P(\mathbf{r};[\rho])$ [82, 83] as

$$V_{T_s}(\mathbf{r};[\rho]) \equiv V_W(\mathbf{r};[\rho]) + V^P(\mathbf{r};[\rho]) \tag{5.1}$$

Since $V_W(\mathbf{r};[\rho])$ is the exact KP for a system where the density can be accurately described by a single orbital, if $V^P(\mathbf{r};[\rho])$ is omitted, one would essentially obtain the ground state density of the corresponding Boson system, where all the electrons are in the same orbital. If we represent the full density by a single orbital function $\psi(\mathbf{r})$,

$$\rho(\mathbf{r}) = \mid \psi(\mathbf{r}) \mid^2 \tag{5.2}$$

then the W KP $V_W(\mathbf{r};[\rho])$ can be written as

$$V_W(\mathbf{r};[\rho]) = -\frac{\bigtriangledown^2\psi(\mathbf{r})}{2\psi(\mathbf{r})} \tag{5.3}$$

One can then combine $V^P(\mathbf{r};[\rho])$ with the one-body potential $V_{eff}(\mathbf{r};[\rho])$ in Eq. (1.3), and derive a Schrödinger-like equation for the Bose orbital $\psi(\mathbf{r})$,

$$\left\{-\tfrac{1}{2}\bigtriangledown^2 + V_{eff}(\mathbf{r};[\rho]) + V^P(\mathbf{r};[\rho])\right\}\psi(\mathbf{r}) = \mu\psi(\mathbf{r}). \tag{5.4}$$

In other words, $V_{eff}(\mathbf{r};[\rho]) + V^P(\mathbf{r};[\rho])$ is now the one-body effective potential for the corresponding Boson system with the same electron density. This reduction of an N-fermion problem to a Boson form is widely implemented in OF-DFT due to

its numerical stability and its easy implementation using existing KS-DFT codes [16].

The associated Pauli potentials for the LQ ($\alpha = 1/2$) and HQ ($\alpha = 2/3$) KPs are immediately obtained by subtraction of the W KP from Eq. (4.16) and Eq. (4.11) respectively,

$$V_\alpha^P(\mathbf{r};[\rho]) = V_{TF}(\mathbf{r};[\rho]) + \frac{2}{3\alpha} V_\alpha^{nloc}(\mathbf{r};[\rho], k_F(\mathbf{r})). \tag{5.5}$$

Similarly, the associated Pauli potentials for the LHQ KPs can be computed by Eq. (A.9).

The standard finite difference method for solving Euler equations for the TFW models [71] are implemented for the LQ, HQ, and LHQ models, and the nonlocal terms are evaluated by Fourier transforms. The code uses the finite difference method with the Gauss-Chebyshev (of the second kind) radial quadrature (for both the grids in the real and reciprocal space), proposed by Becke *et al.*, consisting of 1000 points, and Becke's algorithms for solving Poisson's equation for the Hartree potential [74]. The total energy for the LQ, HQ, and LHQ models is computed by Eq. (4.23), and that for the LHQ models is computed by Eq. (A.8).

As shown in Table 5.1, the atomic energy calculated by the LQ, HQ, and LHQ models is close to the KS-DFT, and is much better than that predicted by the TF1/9W and TFW models. In Table 5.2, we compare the electron density at the nucleus $\rho(0)$ with various models. The TF1/9W model overestimates $\rho(0)$ by about a factor of 10, while the TFW model underestimates it by about 30%. The

Table 5.1: Atomic energy E using the TFλW models, the KS method and the LQ, HQ, and LHQ models in all-electron calculation.

	KS	LQ	HQ	LHQ	$TF1/9W$	TFW
He	-2.834	-2.565	-2.437	-2.560	-3.324	-1.559
Ne	-128.2	-134.3	-126.6	-134.0	-140.6	-86.40
Ar	-525.9	-545.9	-512.2	-545.6	-563.2	-375.5
Kr	-2750	-2805	-2621	-2807	-2900	-2099
Xe	-7229	-7306	-6844	-7314	-7564	-5701
Be	-14.45	-14.39	-13.64	-14.36	-16.40	-8.699
Mg	-199.1	-207.9	-195.7	-207.6	-216.1	-136.4
C	-37.42	-38.97	-36.85	-38.87	-42.29	-24.01
N	-54.02	-56.71	-53.59	-56.59	-60.72	-35.33
O	-74.47	-78.39	-74.02	-78.24	-83.12	-49.39
Si	-288.2	-300.4	-282.5	-300.1	-311.0	-200.5
P	-339.9	-354.1	-332.7	-353.7	-366.1	-238.3
S	-396.7	-412.8	-387.7	-412.5	-426.4	-279.9

Table 5.2: Electron density at the nucleus $\rho(0)$, using the TFλW models, the KS method and the LQ, HQ, and LHQ models in all-electron calculations.

	KS	LQ	HQ	LHQ	$TF1/9W$	TFW
He	3.525	3.088	2.742	3.070	50.81	0.9515
Ne	614.5	576.6	517.6	573.0	6538	169.6
Ar	3819	3642	3282	3621	3.858×10^4	1093
Be	34.86	30.49	27.17	30.29	410.3	8.952
Mg	1086	1024	920.9	1018	1.134×10^4	303.0
C	126.0	113.3	101.2	112.5	1397	33.07
N	203.9	185.6	166.1	184.4	2225	54.24
O	308.6	284.1	254.6	282.3	3331	83.19
Si	1754	1662	1495	1652	1.806×10^4	493.9
P	2173	2062	1857	2050	2.225×10^4	614.5
S	2654	2523	2272	2508	2.703×10^4	753.5

Figure 5.1: Radial density $r^2\rho$ of the Kr atom using the TFλW models, the KS method and the LQ, HQ, and LHQ models with the full nuclear potential.

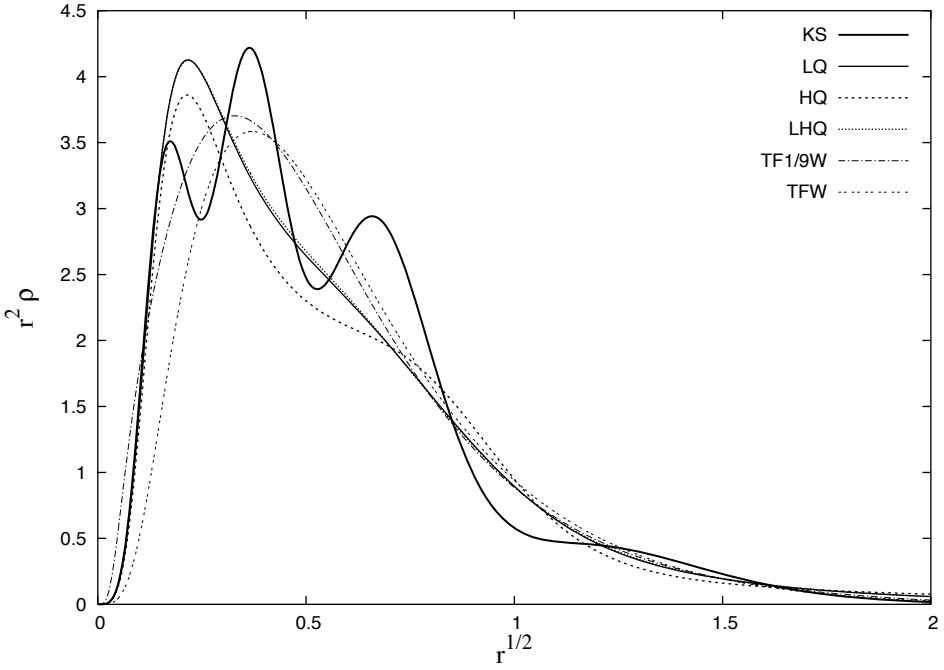

predicted values of $\rho(0)$ for both of the LQ, HQ, and LHQ models are very close to the KS results.

In Figs. 5.2 and 5.2, we compare the radial density distribution $r^2\rho(r)$ of the LQ, HQ, and LHQ models to that predicted by other theories. Using the full Coulombic potential, all the LQ, HQ, and LHQ models can predict an incipient shell structure for heavy atoms ($Z \gtrsim 30$). Both the TF1/9W and TFW models predict smooth and structureless radial density profiles. Since the full Coulombic potential is certainly far beyond the LR regime, and the total atomic density $\rho(r)$ is large and rapidly varying near the nucleus, these qualitatively reasonable results with some suggestion of shell structure are about as good as could be hoped for, and compare favorably to most previous OF theories. However, the difference in the results for

Figure 5.2: Same as in Fig. but for the Xe atom

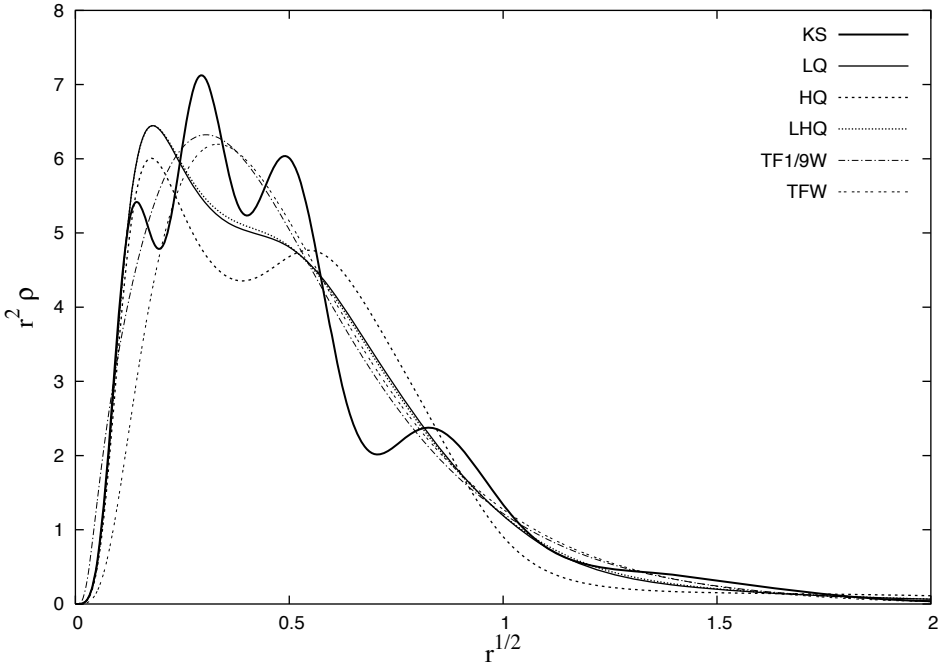

the LQ, HQ, and LHQ models indicates that the OF theory is being used outside its range of validity. As shown below, we gain a significant improvement by using the AILPS to deal with these difficulties.

5.2.2 *Ab initio* local pseudopotential calculation

To determine $\rho_v(\mathbf{r})$ for the reference systems constructed in Chapter 4, the Euler equation (4.33) can be transformed to a Schrödinger-like equation

$$\left\{-\tfrac{1}{2}\nabla^2 + V_H(\mathbf{r};[\rho_v]) + V_{xc}(\mathbf{r};[\rho_v]) \right. \\ \left. + V_{ext}(\mathbf{r}) + V_P(\mathbf{r};[\rho_v])\right\}\psi_v(\mathbf{r}) = \mu\psi_v(\mathbf{r}) \tag{5.6}$$

where

$$\rho_v(\mathbf{r}) = \mid \psi_v(\mathbf{r}) \mid^2 . \tag{5.7}$$

For an atomic system, $V_{ext}(\mathbf{r}) = V_{ps}(\mathbf{r})$ is given as input data. The valence

Table 5.3: The total energy E for reference systems using the KS method and the LQ, HQ, and LHQ models.Parameters used in Eq. (4.30) for such systems are given in Table 4.1.

	E_{KS}	E_{LQ}	E_{HQ}	E_{LHQ}	$E_{TF1/9W}$	E_{TFW}
Be	-0.9914	-0.8955	-0.8950	-0.8979	-1.408	-0.7786
C	-6.134	-6.080	-6.100	-6.086	-8.881	-5.266
N	-11.04	-11.06	-11.09	-11.07	-15.91	-9.462
O	-18.01	-18.09	-18.09	-18.08	-25.57	-15.30
Si	-3.771	-3.738	-3.750	-3.743	-4.833	-3.350
P	-6.474	-6.432	-6.455	-6.436	-7.889	-5.756
S	-10.20	-10.10	-10.14	-10.10	-11.94	-9.023
Ar	-21.37	-20.84	-20.91	-20.83	-22.19	-18.56

density $\rho_v(\mathbf{r})$ predicted by the OF KPs is determined from Eqs. (5.6) and (5.7), and can be directly compared to the exact target density $\tilde{\rho}_v(\mathbf{r})$ given by the full KS theory. Table 4.1 shows the parameters used to construct the reference systems of atoms, and Table 5.3 shows the total energy values for such systems using the KS-DFT, and the LQ, HQ, and LHQ models. As can been seen, the agreement of the LQ, HQ and LHQ models with the KS-DFT are excellent.

Fig. 4.2 shows the three parameterized valence density $\tilde{\rho}_v(r)$ of the Si pseudoatom, along with the total KS density $\rho_{KS}(r)$. It can be seen that $\rho_{KS}(r)$ increases rapidly for $r < r_c$, and reaches a very large value at the nucleus, $\rho_{KS}(0) = 1754$, for example, more than a hundred thousand times larger than the proposed pa-

Figure 5.3: The smooth valence density $\tilde{\rho}_v(r)$ from Eq. (4.30), with parameters given in Table 4.1 for the Si pseudoatom used in the inverse-KS process, and the valence density $\rho_v(r)$ predicted by the LQ, HQ , and LHQ models using the $V_{ps}(r)$ (see Fig. 4.3) corresponding to $\tilde{\rho}_v(r)$. The arrow indicates the location of r_c.

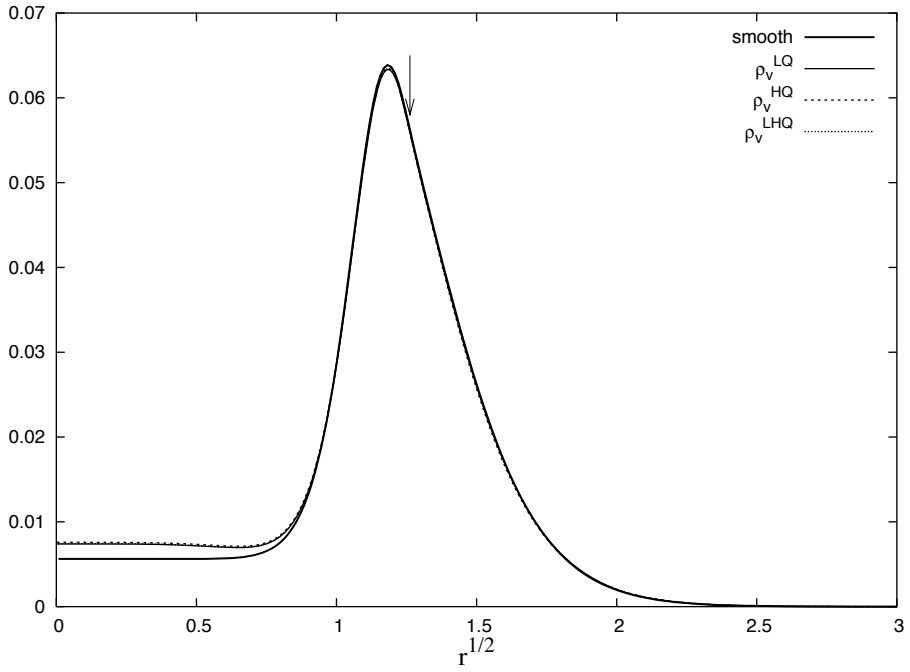

Figure 5.4: Radial density $r^2\rho$ of the Si atom using the full KS method and various models using AILPS. Parameters used for constructing this reference system are shown in Table 4.1. The arrow indicates the location of r_c.

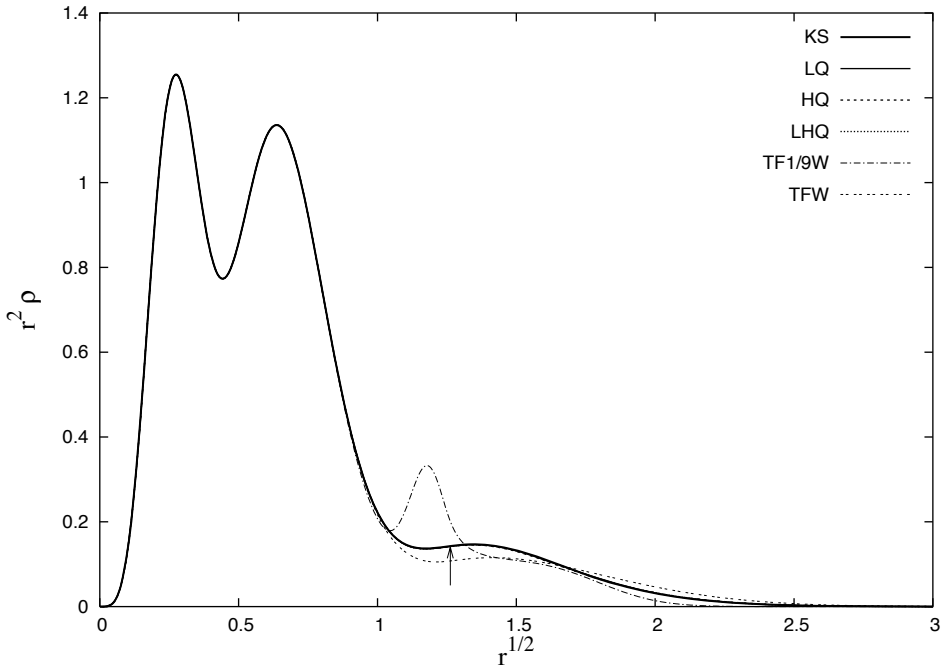

Figure 5.5: Same as in Fig. 5.4 but for the N atom.

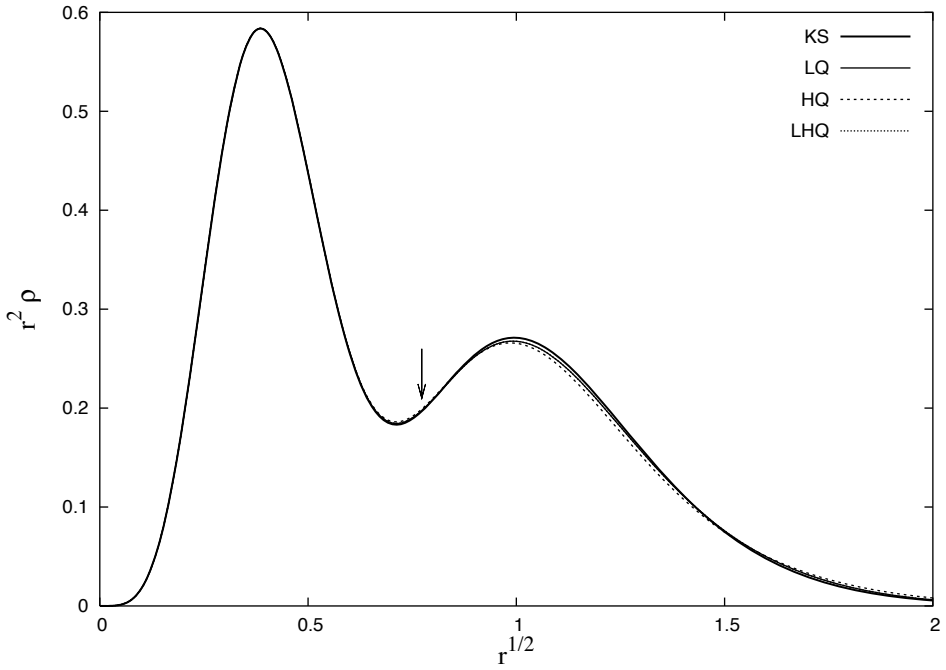

Figure 5.6: Same as in Fig. 5.4 but for the Be atom.

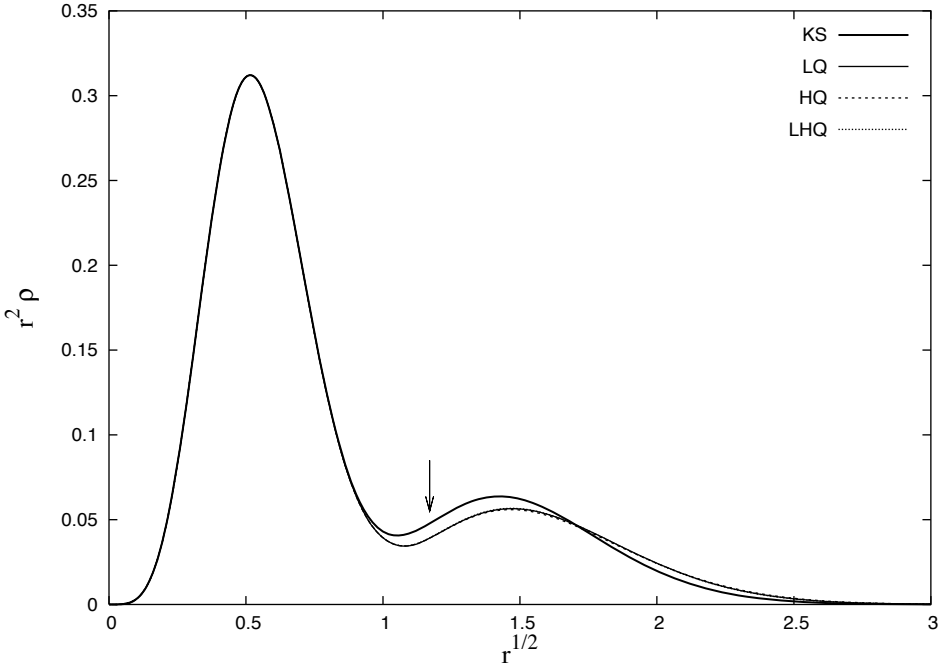

Figure 5.7: Same as in Fig. 5.4 but for the Ar atom.

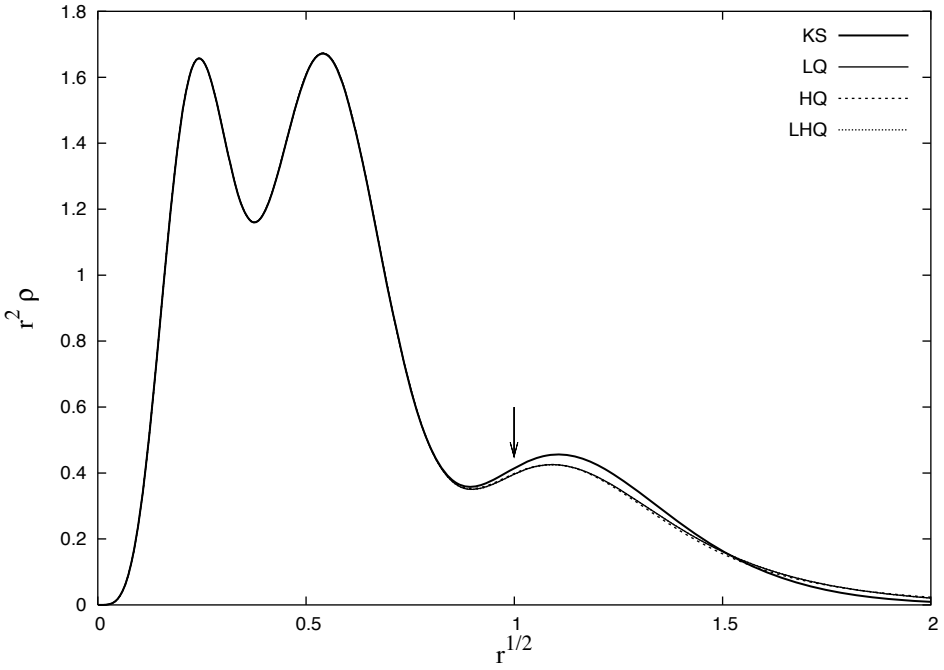

Figure 5.8: Ionization energies of the first and the second row atoms using the full KS method, and various models using AILPS. For Ar, the TF1/9W model fails to predict a positive ionization energy ($I = -1.010$).

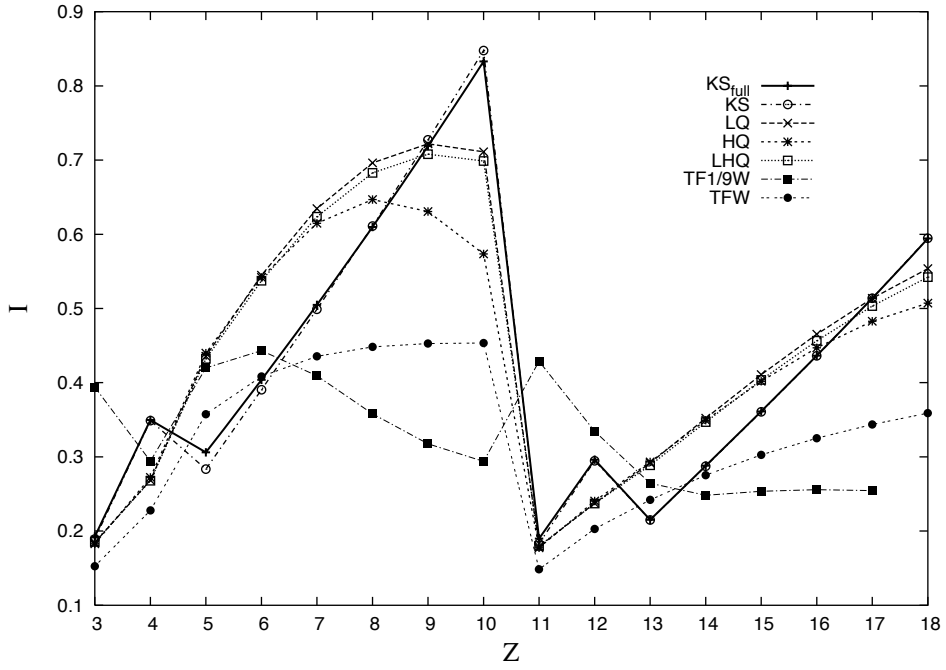

rameterized valence density $\tilde{\rho}_v(0) = 0.005621$ (for $p = q = 6$). Fig. 4.3 shows the corresponding AILPS generated by the three parameterized valence density in Fig. 4.2.

Fig. 5.3 shows the input valence density $\tilde{\rho}_v(r)$ used in the inverse-KS process, and the predicted valence density $\rho_v(r)$ given by the LQ and HQ models, obtained using the input $V_{ps}(r)$ shown in Fig. 4.3. Because of the weak $V_{ps}(r)$ and the slowly varying valence density, both the LQ and HQ models predict results very close to those of the exact KS theory. The predicted radial density of atoms are shown in Figs. (5.4 – 5.7). The resulting clear shell structure is in excellent agreement with the full KS-DFT calculations and shows that the OF treatment of the valence density does not produce noticeable errors in the core region. The consistency of our OF theory when pseudopotentials are used is illustrated by the great similarity of the density predicted by the different HQ and LQ models. Their slight deviation from the KS-DFT results might be due to the inappropriate form for the TBFWV $k_F(\mathbf{r}, \mathbf{r}') = k_F(\mathbf{r})$ in these models, even when the local pseudopotential is within LR regime.

For a simple test on the transferability of the present AILPS, we perform calculations on ions. Fig. 5.8 shows the ionization energies of various atoms, using various models. As can be seen, the ionization energies from the full KS-DFT and from the KS-DFT with AILPS are quite similar. Therefore, the present AILPS is quite transferable to these positive ions. The LQ, HQ, LHQ models can capture the overall periodicity of ionization energies, while other OF models perform badly.

5.3 Molecules

The OF-DFT has not been widely applied to molecular systems, possibly due to its lack of sufficient accuracy, when compared with the KS-DFT. It has been known that the classical TF model (without $E_{xc}[\rho]$) predicts no binding of molecules, and including the Dirac exchange energy functional (LDA on $E_x[\rho]$ only), the so-called TFD model, does not improve the situation [1, 33, 36]. To investigate whether $T_W[\rho]$ is responsible for the bonding of molecules, Chan *et al* [36] recently applied the TFDW models to both atoms and diatomic molecules, and they found that there is no single value of λ that provides good results in both atoms and diatomic molecules. The TFDW models can be regarded as using the TFλW KEDFs and LDA on the $E_x[\rho]$ only. However, correlation energy plays an important role in molecular bonding [1], so we use LDA on $E_{xc}[\rho]$ here for all the OF models.

Since diatomic molecules are the simplest of all molecules, we applied the LQ and HQ KPs to such systems, and compared our results to the those from TFλW models, as well as the accurate KS orbital method, and to experimental results. In addition, the AILPS is used for all the OF models to enhance their performance. The KS results are from many papers, and are all based on the local-spin-density approximation (LSDA) on the E_{xc}, a generalization of LDA with spin-dependent densities. To see the sensitivity of binding energies, these results are also compared with experiment. This appears to be the first attempt to apply the LR-based OF-DFT to molecular systems.

If the centers of atoms A and B in a diatomic molecules are separated by a

distance R, they experience an internuclear repulsion, an attraction between the nucleus of one and the electrons of the other, and an interelectronic repulsion. The binding energy of diatomic molecules is the energy difference between the energy of molecules $E(AB)$ and the sum of the energy of the two separate atoms ($E(A)$ and $E(B)$).

The external potential is the linear combination of the atomic pseudopotentials (same as those constructed in Table 4.1) centered at atoms A and B.

$$V_{ext}(\mathbf{r}) = V_{ps}^{A}(\mathbf{r}_A) + V_{ps}^{B}(\mathbf{r}_B) \tag{5.8}$$

Here, $\mathbf{r}_A = \mathbf{r} - \mathbf{R}_A$ and $\mathbf{r}_B = \mathbf{r} - \mathbf{R}_B$. The valence density $\rho_v(\mathbf{r})$ predicted by the OF-DFT is determined by a Schrödinger-like equation in Eqs. (5.6, 5.7). Following Chan *et al*'s approach [36], we use a linear combination of atomic orbitals (LCAO) method, in which the molecular orbital $\psi_v(\mathbf{r})$ in Eq. (5.7) is expanded in atomic orbitals [$\chi_k(\mathbf{r})$: $k = 1, 2, ...$]

$$\psi_v(\mathbf{r}) = \sum_k c_k \chi_k(\mathbf{r}) \tag{5.9}$$

where Cartesian Gaussian-type atomic orbitals are used as the basis function χ_k in the molecular-orbital calculations. To further reduce the cost in computing the matrix elements of $V_H(\mathbf{r};[\rho_v])$ and $V_{xc}(\mathbf{r};[\rho_v])$, we fit $\rho_v(\mathbf{r})$ and $V_{xc}(\mathbf{r};[\rho_v])$ to an auxiliary basis [84]. For the LQ and HQ KPs, we need to evaluate their nonlocal terms on grids, and fit them to an auxiliary basis for the efficient evaluation of matrix elements. Since this nonlocal term is relatively small compared with the

TF and the W KPs, and is also computationally expensive, we describe a scheme to evaluate this nonlocal term accurately and efficiently in Appendix B. This completes the description of our numerical methods for the OF models.

Since a diatomic molecule is symmetric with respect to rotations about the molecular axis, the density is independent of azimuthal angle. Therefore, we only consider s, p_z, and d_{zz} Gaussians in the basis functions, where z is the molecular axis. The exponents in the Gaussian basis functions are chosen as a series m^t; for s Gaussians, we take $m = 2$, $t = -3, -2, ..., 21$, for p Gaussians, we take $m = 2$, $t = -9, -8, ..., 4$, and for d Gaussians, we take $m = 2$, $t = -9, -8, ..., -3$. This is a $25s14p7d$ basis on each atom, which gives a total of 92 basis functions for the diatomic molecule. The range of these exponents of each Gaussians is about the same as that proposed in Chan's paper [36]. The same Gaussian basis functions are used to expand ψ_v, and those fitted functions mentioned above.

We calculated the bond lengths r_e and the binding energy D_e of several diatomic molecules on the first and the second row. The results are compared with the TFW model, the KS-DFT, and experimental results. In the KS calculations, the local-spin-density approximation (LSDA) are used for E_{xc}, a generalization of KS-LDA that allows different orbitals and densities for electrons with different spins. In our OF-DFT, we ignore this spin-dependence effect, since the kinetic energy is on an order of magnitude larger than the exchange-correlation energy.

As can been seen in Table 5.4 and 5.5, the LQ and HQ models perform better than the TFW model. The remaining errors in the LQ and HQ models could be due to the accuracy of the KPs, the transferability of AILPS, and the ignoring

Table 5.4: Bond lengths r_e of the diatomic molecules. The KS results are from Becke [74], except for the CO and NO molecules, which are from Dhar *et al* [85]. The experimental results are from Huber [86], except the CO, and NO molecules, which are from Baerends *et al* [87].

	$Expt$	KS	LQ	HQ	TFW
H_2	1.40	1.45	2.1	2.1	3.2
C_2	2.35	2.35	2.2	2.2	2.6
N_2	2.07	2.10	1.9	2.0	2.2
Si_2	4.24	4.29	3.9	4.0	4.7
P_2	3.58	3.57	3.8	3.8	4.4
S_2	3.57	3.57	4.0	3.8	4.1
Cl_2	3.76	3.74	3.9	3.7	3.8
CO	2.13	2.14	2.0	2.0	2.3
NO	2.17	2.18	1.9	1.9	2.1

Table 5.5: Binding energies $D_e = E(A) + E(B) - E(AB)$ (eV) of the diatomic molecules. The KS and the experimental results are from the same papers in Table 5.4.

	$Expt$	KS	LQ	HQ	TFW
H_2	4.8	4.9	1.0	1.5	1.9
C_2	6.3	7.3	17.0	19.5	18.0
N_2	9.9	11.6	17.5	22.7	22.2
Si_2	3.1	4.0	3.6	4.4	5.8
P_2	5.1	6.2	3.2	5.1	7.8
S_2	4.4	5.9	2.8	5.2	9.4
Cl_2	2.5	3.6	2.1	4.9	10.8
CO	11.2	11.1	15.0	22.8	23.5
NO	6.6	6.7	14.6	23.6	23.8

Figure 5.9: Binding curve of C_2 using the TFW model and the LQ and HQ KPs.

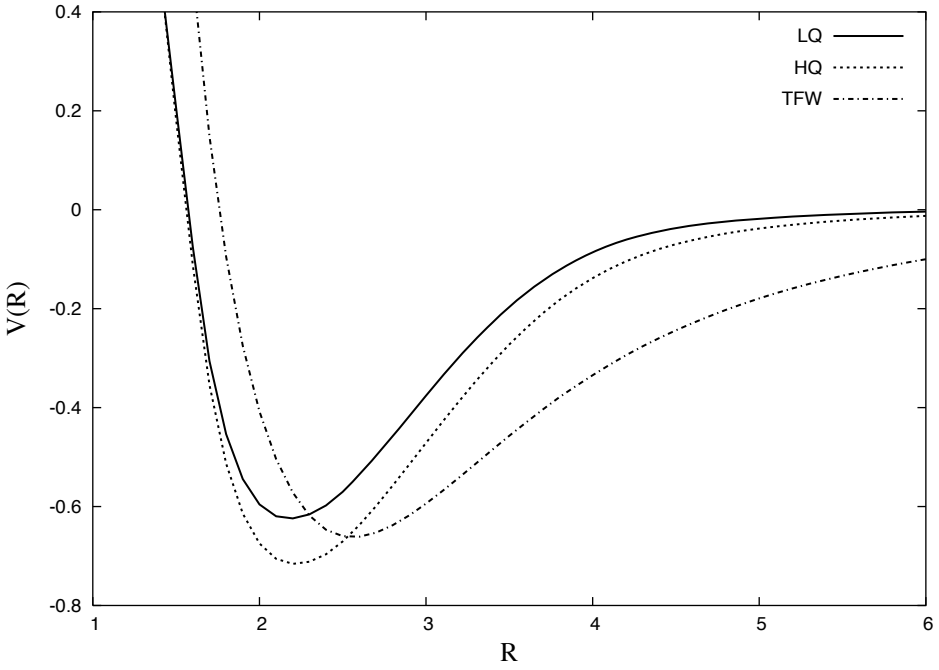

Figure 5.10: Same as in Fig. 5.9 but for N_2

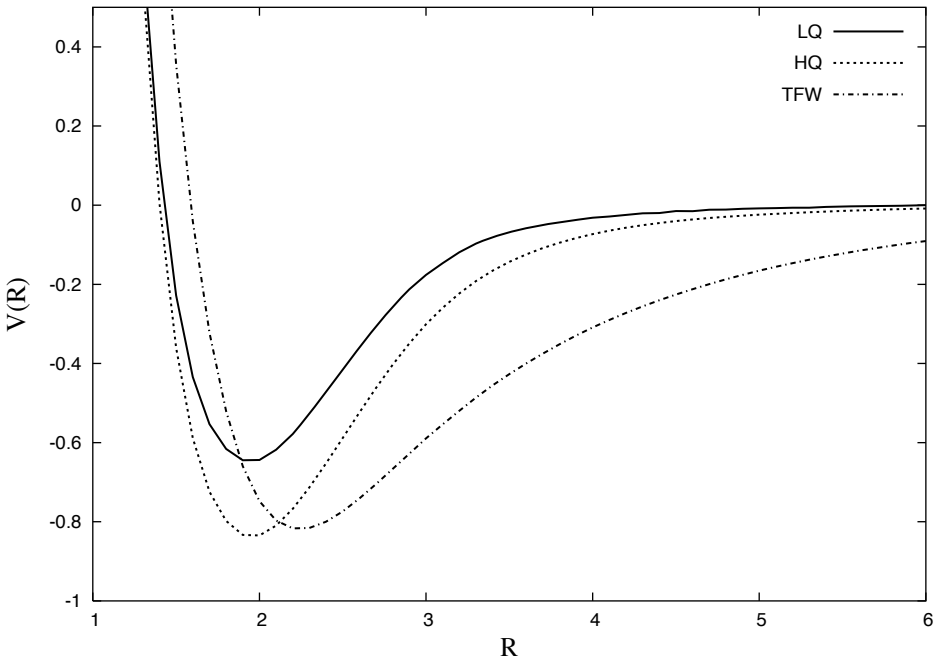

Figure 5.11: Same as in Fig. 5.9 but for Cl_2

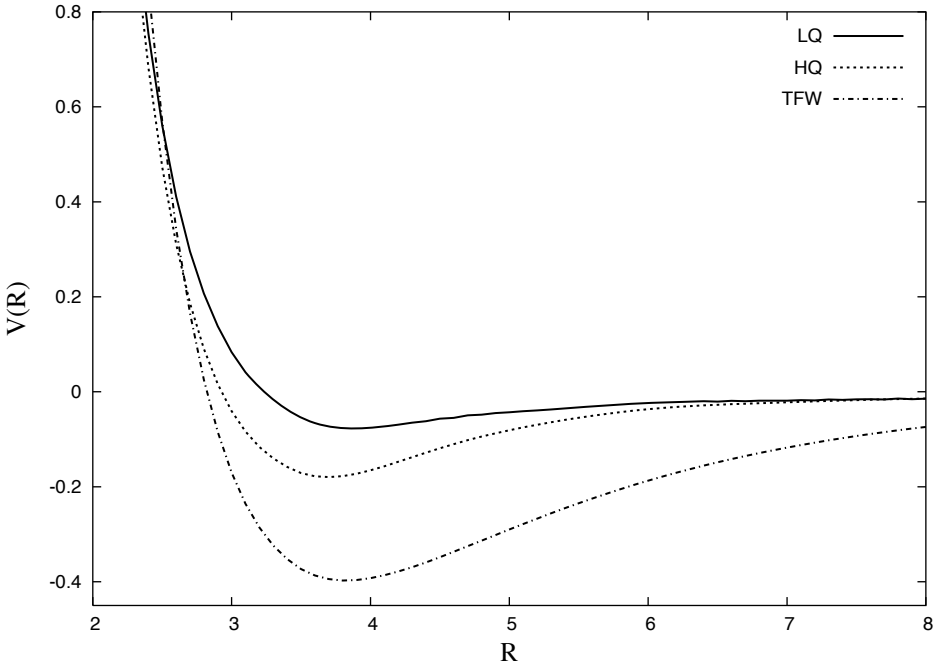

Figure 5.12: Same as in Fig. 5.9 but for CO

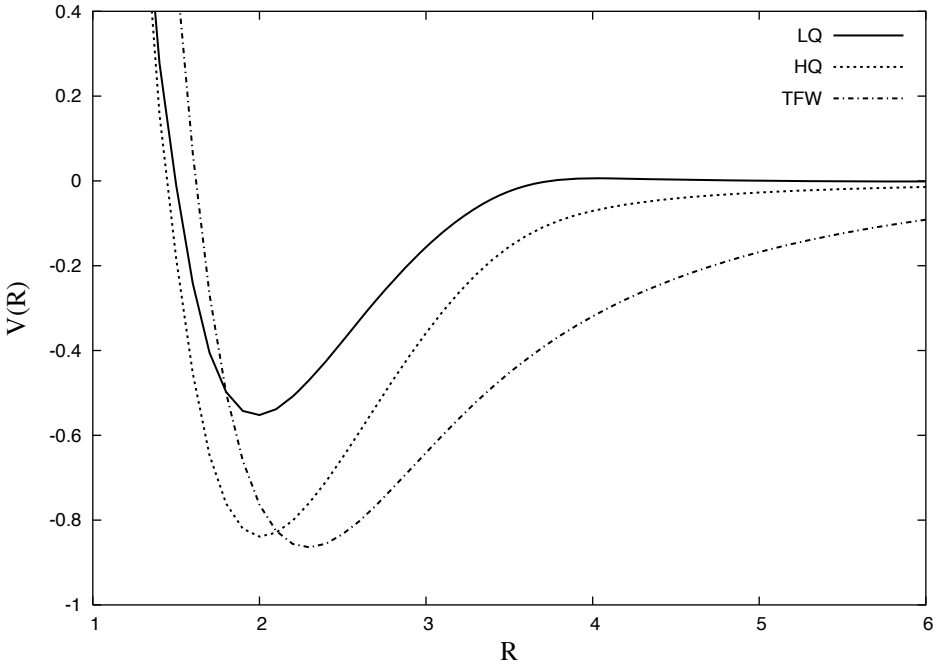

of spin in $E_{xc}[\rho]$. As can be seen, even the KS-LSDA calculations show some noticeable deviations in the binding energies of diatomic molecules from experimental results. Therefore, the binding energies of diatomic molecules are sensitive to any approximations used on E_{xc}.

The binding curve of some diatomic molecules are shown Figs. (5.9 – 5.12). The LQ and HQ results are similar for both small and large R, but show deviations in the intermediate R, especially in the bond length. Their discrepancy indicates that choices of the TBFWV ($k_F(\mathbf{r}, \mathbf{r}') = k_F(\mathbf{r})$ used in the LQ and HQ KPs) is sensitive in diatomic molecules, even when a weak and slowly varying AILPS is used. Therefore, we do not expect that the LHQ KPs would perform better than the LQ and HQ KPs in such cases. However, their improvements in both of the bond lengths and the binding energies from the local TFW model, suggests that the nonlocal terms in our proposed LR-based KPs are indeed important to give good qualitative results.

5.4 Solids

The research in this section is in collaboration with Prof. Emily A. Carter's group at Princeton University. The calculations were performed on their Wiffin Cluster. We are grateful for their computational support.

In solids, the external potential $V_{ext}(\mathbf{r})$ is a linear combination of the special array of the local atomic pseudopotentials centered at each ion position $\mathbf{R}_I$ (see Eq. (4.32)). Different arrays of $\mathbf{R}_I$ lead to different phases, such as face-centered cubic

Table 5.6: Lattice parameters ($\mathring{A}$) for bulk Al.

Al	KS	LQ	HQ	LHQ	WT	WGC
fcc	4.03	4.04	4.04	4.04	4.04	4.03
bcc	3.23	3.23	3.23	3.23	3.23	3.22
sc	5.33	5.31	5.36	5.31	5.33	5.38
dia	5.84	5.91	5.90	5.91	5.94	5.92

(fcc), diamond (dia), body-centered cubic (bcc), simple cubic (sc), and so on.

For periodic systems, such as solid-state systems, the KS-DFT scales as $O(N_k \cdot N^3)$, where N_k is the number of the $\mathbf{k}$ points used for the Brillouin-zone (BZ) sampling, and N is the number of atoms. For metallic systems, this BZ sampling is very expensive, and N_k can be on the order of 1000. The use of OF-DFT, however, can eliminate such a sampling, and also maintains the linear scaling. As a result, the OF-DFT is computationally more suitable to study very large systems, especially metallic systems, than KS-DFT. Further development of OF-DFT may improve its performance for many different systems. Here, we study two very different materials, a nearly-free-electron-like metal (solid Al) and a covalent material (solid Si), using the proposed nonlocal KPs, and compare our results with other KEDFs and the KS-DFT.

For bulk Al, the empirical Goodwin-Needs-Heine (GNH) local pseudopotential for aluminum [88] is used, and the plane wave cutoff up to 600 eV is used to converge the electron density. We apply the linear scaling version of the LQ, HQ and LHQ KPs, and expand the kernel to the zeroth order, and let $\rho_* = \rho_0$ in the calculations.

Table 5.7: Energy per atom (eV) for bulk Al. The first row is the energy for the fcc structure, while other rows are energy difference from the fcc structure.

Al	KS	LQ	HQ	LHQ	WT	WGC
fcc	-58.336	-58.303	-58.314	-58.302	-58.331	-58.331
bcc	0.068	0.053	0.057	0.053	0.060	0.066
sc	0.250	0.253	0.253	0.254	0.227	0.217
dia	0.599	0.712	0.751	0.720	0.673	0.584

Table 5.8: Lattice parameters ($\mathring{A}$) for bulk Si.

Si	KS	LQ	HQ	LHQ	WGC
dia	5.38	5.27	5.29	5.27	5.77
bcc	3.29	3.06	3.06	3.06	3.29
sc	4.99	4.98	4.98	4.98	5.01
fcc	3.83	3.83	3.82	3.83	3.80

Table 5.9: Energy per atom (eV) for bulk Si. The first row is the energy for the dia structure, while other rows are energy difference from the dia structure.

Si	KS	LQ	HQ	LHQ	WGC
dia	-110.234	-109.167	-109.282	-109.161	-110.345
bcc	0.165	-0.553	-0.437	-0.558	0.537
sc	0.303	-0.586	-0.531	-0.587	0.506
fcc	0.457	-0.584	-0.478	-0.588	0.571

The linear density pathway is used for computing the kinetic energy of LQ, HQ, and LHQ models (see Chapter 4). Our results are compared with the WT [26] and WGC [15] KEDFs, and the KS-DFT, which were previously computed [15], using the same type of local pseudopotential. As can been seen in Table 5.6 and 5.7, all the LR-based models perform similarly, and agree well with the KS-DFT. The phase ordering is correct, and the lattice parameters of the four phases are close to the KS results.

For bulk Si, the bulk local pseudopotential (BLPS) developed by Zhou *et al* [17] is used, and the plane wave cutoff up to 2000 eV is used to converge the electron density. We carry out the linear scaling method to our nonlocal KPs to the first order, and let $\rho_* = \rho_0$. Our results are compared with the WGC [15] KEDF, and the KS-DFT, which were previously computed [18], using the same type of local pseudopotential. As can been seen in Table 5.8 and 5.9, the LR-based models perform worse than for Al, when compared with the KS-DFT. The phase ordering is incorrect, and the lattice parameters of the four phases only qualitatively match with the KS results. This disagreement might be due to the inappropriate form for the TBFWV $k_F(\mathbf{r}, \mathbf{r}')$. For example, $k_F(\mathbf{r}, \mathbf{r}') = k_F$ in the WT KEDF, $k_F(\mathbf{r}, \mathbf{r}') = k_F^\gamma(\mathbf{r}, \mathbf{r}') = (\frac{k_F^\gamma(\mathbf{r}) + k_F^\gamma(\mathbf{r}')}{2})^{1/\gamma}$in the WGC KEDF, and $k_F(\mathbf{r}, \mathbf{r}') = k_F(\mathbf{r})$ in the LQ, HQ and LHQ KPs. Since Si is a covalent material, the density outside the covalent bond regions is quite different from the one inside, so the choice of the TBFWV might be sensitive in Si, even when the local pseudopotential is within the LR regime. Further work is definitely called for here.

Chapter 6

Conclusion

In summary, we propose a family of nonlocal OF KPs that satisfy exact limits for small and large wavevector perturbations and reproduce the exact LR function in the homogeneous limit. In general, there is no reason to believe that any LR-based OF-DFT should work well for arbitrary systems, especially when the model potentials are far beyond the LR regime. However, a KP that satisfies the two limiting forms of the exact KP will remain accurate to all orders of the perturbation when the density variations fall into the corresponding limiting regimes, and in those cases will provide high accuracy. Moreover, since only changes of valence electron densities are related to most chemical processes, and the interaction of the core electrons and the nuclei on the valence electrons can be described by a weak AILPS, our use of a LR-based OF-KP together with AILPS is well justified. Since our proposed scheme generates a small $\rho_v(r)$, this also validates our use of the local FWV $k_F(\mathbf{r})$ for the TBFWV $k_F(\mathbf{r}, \mathbf{r}')$ in many cases.

The proposed models are not only conceptually simple, but also exact for a system with a weak potential and a low or slowly-varying density. When the AILPS is used, the atomic densities given the LQ and HQ KPs become virtually indistinguishable from those given by the KS method. The appearance of the atomic shell structure is found to be very sensitive to the accuracy of the proposed KPs.

Fortunately, by using the AILPS, we could reach such accuracy in atomic systems using all the LQ, HQ, and LHQ KPs. In diatomic molecules, the small deviations in the prediction of the LQ and HQ models may indicate the binding energy is very sensitive to the accuracy of the KPs. This can be understood, since even the KS-LDA and KS-LSDA methods, with different exchange-correlation energy functionals, have shown differences from the experimental results. For near-free-electron-like solids, the LR-based OF-DFT works quite well, when compared with the KS-DFT, while it performs less well in covalent materials, such as Si. In general we found that our present versions of LR-based OF-DFT are able to give qualitatively reasonable predictions for a wide variety systems, when compared with the KS-DFT. Therefore, it may be suitable for use in OF-AIMD, and can be applied to systems with a very large number of atoms.

We close this Chapter with some suggestions for future work. Based on our numerical results, we found that the LHQ KPs, which satisfy both the LQ and HQ limits up to second order, do not significantly improve the LQ and HQ KPs. We believe that this is because these LR-based OF models have to rely on an approximate form for the TBFWV. Since the TF KEDF is derived by making local use of results for the uniform electron gas, this approximation could be substantial, and getting the second order terms correct in either the LQ or HQ limits may not necessarily improve the results, even when the AILPS is within the LR regime. This same point also applies to other LR-based KEDFs, such as the WT [26], WGC [15], and SM [22] KEDFs. Therefore, the development of an appropriate LR theory for inhomogeneous systems, with a suitable form for the TBFWV remains an important

goal for future work in OF-DFT. To make progress, one could use a nonlocal $k_F(\mathbf{r}, \mathbf{r}')$ for inhomogeneous systems, similar to the idea of using a nonlocal KEDF or KP. One could follow an approach similar to the one we used here for constructing the nonlocal KPs, and constrain the nonlocal $k_F(\mathbf{r}, \mathbf{r}')$ by requiring that it satisfy certain known limits, rather than simply taking a mathematically convenient and symmetric form, and empirically determining arbitrary fitting parameters. The latter way of constructing $k_F(\mathbf{r}, \mathbf{r}')$ is similar to the way workers originally tried to determine the "best" λ for the TFλW models, and more systematic LR-based approaches have provided significant improvements.

In addition to seeking an appropriate $k_F(\mathbf{r}, \mathbf{r}')$, one could also try to reduce the computational cost from the typical quadratic scaling (from the nonlocal terms in KPs) to linear scaling, as discussed in Chapter 4. In our approach, an accurate pathway to compute the kinetic energy is needed. For extended systems, developing a generalized Herring's pathway may be helpful, since only this pathway satisfies the exact scaling relation of the KEDF.

Finally, in previous studies of OF-DFT, conclusions were usually drawn from the results on specific systems studied by KEDFs with empirical parameters fit to those systems. Therefore, these conclusions may not be generally applicable. For example, the empirically constructed TF1/5W model (the best TFλW model for atoms) gives poor binding energies and bond lengths for diatomic molecules [36]. Another example is that the best γ-parameter in the WGC KEDF for Al is not the optimal one for Si. In this dissertation, we have presented the first attempt to apply the same LR-based OF-DFT to study a very wide range of systems: atoms,

molecules, and solids. This provides a severe test for any such theory, and helps uncover deficiencies in the present formulation. Further work along these lines could lead to a generally accurate OF-DFT.

Appendix A

LHQ Kinetic Potentials

In order to construct a KP that satisfies both of the LQ and HQ limits up to second order, here we propose the following trial KP using a linear combination of $V_\alpha^{nloc}(\mathbf{r};[\rho],k_F(\mathbf{r}))$ with two different α's.

$$\begin{aligned} V_{\{\alpha_1,\alpha_2\}}(\mathbf{r};[\rho],k_F(\mathbf{r})) &= V_{TF}(\mathbf{r};[\rho]) + V_W(\mathbf{r};[\rho]) \\ &\quad +\gamma_1\ V_{\alpha_1}^{nloc}(\mathbf{r};[\rho],k_F(\mathbf{r})) \\ &\quad +\gamma_2\ V_{\alpha_2}^{nloc}(\mathbf{r};[\rho],k_F(\mathbf{r})) \end{aligned} \tag{A.1}$$

To satisfy the LR theory of uniform systems, and the LQ and HQ limits up to second order, only certain sets of these parameters are satisfied. From the limits of $\hat{f}(q)$ in Eq. (4.15) and $V_\alpha^{nloc}(\mathbf{r};[\rho],k_F(\mathbf{r}))$ in Eq. (4.16), and the following relation [13],

$$\frac{\nabla^2\rho^\alpha}{\rho^\alpha} = \left\{\alpha(\alpha-1)\frac{|\nabla\rho(\mathbf{r})|^2}{\rho(\mathbf{r})^2} + \alpha\frac{\nabla^2\rho(\mathbf{r})}{\rho(\mathbf{r})}\right\}. \tag{A.2}$$

we obtain the following three relations for the possible α_1, α_2, γ_1, and γ_2.

$$\gamma_1 = -\frac{1}{9(\alpha_1^2 - \frac{4}{3}\alpha_1 + \frac{1}{3})} \tag{A.3}$$

$$\gamma_2 = 1 - \gamma_1 \tag{A.4}$$

and

$$\alpha_2 = \frac{\frac{2}{3} - \gamma_1\alpha_1}{1 - \gamma_1} \tag{A.5}$$

Without loss of generality, let $\alpha_1 \leq \alpha_2$. Since α_1 and α_2 are positive, the acceptable range of α_1 is

$$0 < \alpha_1 < 1/3 \tag{A.6}$$

and

$$2/3 < \alpha_1 < 1 \tag{A.7}$$

The latter in Eq. (A.7) is, however, unstable from several numerical tests in atoms, so only the former in Eq. (A.6) will be adopted. Since this types of KPs in Eq. (A.1) satisfy both the LQ and HQ limits up to second order, we denote this type of kinetic potentials as $V_{LHQ\{\alpha_1\}}$ KPs, where α_1 satisfies Eq. (A.6), and α_2, γ_1, and γ_2 are determined from Eqs. (A.3, A.4, and A.5).

The Kinetic energies of the LHQ KPs using the Herring's pathways are:

$$\begin{aligned} T_{\alpha_1}^{LHQ}[\rho] &= T_{TF}[\rho] + T_W[\rho] \\ &\quad + \int d\mathbf{r} \int d\mathbf{r}'(\gamma_1 V_{\alpha_1}^{nloc}(\mathbf{r};[\rho], k_F(\mathbf{r})) + \gamma_2 V_{\alpha_2}^{nloc}(\mathbf{r};[\rho], k_F(\mathbf{r})) \\ &\quad \times \bigtriangledown \cdot (\mathbf{r}\rho(\mathbf{r})) \end{aligned} \tag{A.8}$$

Similarly, the Kinetic energies of the LHQ KPs using the linear density pathway, can be computed in a way similar to that of the LQ and HQ KPs (see Chapter

4).

The Pauli potentials (see Chapter 5) for the LHQ KPs are:

$$V^P_{LHQ\{\alpha_1\}}(\mathbf{r};[\rho]) = V_{TF}(\mathbf{r};[\rho]) + \gamma_1 V^{nloc}_{\alpha_1}(\mathbf{r};[\rho],k_F(\mathbf{r})) + \gamma_2 V^{nloc}_{\alpha_2}(\mathbf{r};[\rho],k_F(\mathbf{r})). \quad \text{(A.9)}$$

Appendix B

Numerical Methods for Efficiently Computing the Nonlocal Kinetic Potentials of Diatomic Molecules Using Gaussian Basis Functions

The nonlocal terms in LQ (in Eq. (4.16)), HQ (in Eq. (4.11)), and LHQ (in Eq. (A.1)) KPs can be written as the following general form:

$$V_{nl}(\mathbf{r}) = h(\mathbf{r}) \int f(|\mathbf{r}-\mathbf{r}'|; k_F(\mathbf{r}))\ g(\mathbf{r}'; [\rho_v]) d\mathbf{r}' = \frac{h(\mathbf{r})}{(2\pi)^3} \int \hat{f}(k/2k_F(\mathbf{r}))\ g(\mathbf{k}) e^{-i\mathbf{k}\cdot\mathbf{r}} d\mathbf{k} \tag{B.1}$$

Our task is to evaluate it on grids, and then obtain its matrix element as discussed before. One might evaluate this integral numerically. However, even with the symmetry of diatomic molecules, the total cost for doing this is still $O(N_r N_\theta N_k N_{k_\theta})$. Here, we use the property of Gaussians to simply the evaluation of this nonlocal term.

First, we fit $g(\mathbf{r})$ to a Gaussian basis set, and write it into sum of two different centered basis sets:

$$g(\mathbf{r}) = \sum_l c_l^A \chi_l^A(\mathbf{r}_A) + \sum_m c_m^B \chi_m^B(\mathbf{r}_B) \tag{B.2}$$

Here, $\mathbf{r}_A = \mathbf{r} - \mathbf{R}_A$ and $\mathbf{r}_B = \mathbf{r} - \mathbf{R}_B$. Using property of the Fourier transform, $V_{nl}(\mathbf{r})$ can be written as sum of two Fourier transforms centered at $\mathbf{R}_A$ and $\mathbf{R}_B$ respectively. Then, it becomes

$$V_{nl}(\mathbf{r}) = \frac{h(\mathbf{r})}{(2\pi)^3}\sum_l c_l^A \int \hat{f}(k/2k_F(\mathbf{r}))\ \chi_l^A(\mathbf{k})e^{-i\mathbf{k}\cdot\mathbf{r}_A}d\mathbf{k} + \frac{h(\mathbf{r})}{(2\pi)^3}\sum_m c_m^B \int \hat{f}(k/2k_F(\mathbf{r}))\ \chi_m^B(\mathbf{k})e^{-i\mathbf{k}\cdot\mathbf{r}_B}d\mathbf{k} \tag{B.3}$$

As discussed before, due to the cylindrical symmetry of diatomic molecules, we only consider the s, p_z, and d_{zz} Gaussians, where z is the molecular axis. Their Fourier transforms are

$$\chi_l^{A,S}(\mathbf{r}) = \exp[-\alpha_l r_A^2] \implies \chi_l^{A,S}(\mathbf{k}) = (\frac{\pi}{\alpha_l})^{3/2}\exp[-\frac{k^2}{4\alpha_l}] \tag{B.4}$$

$$\chi_l^{A,P_Z}(\mathbf{r}) = z_A\exp[-\alpha_l r_A^2] \implies \chi_l^{A,P_Z}(\mathbf{k}) = i\frac{k_Z}{2\alpha_l}(\frac{\pi}{\alpha_l})^{3/2}\exp[-\frac{k^2}{4\alpha_l}] \tag{B.5}$$

$$\chi_l^{A,D_{ZZ}}(\mathbf{r}) = z_A^2\exp[-\alpha_l r_A^2] \implies \chi_l^{A,D_{ZZ}}(\mathbf{k}) = (\frac{\pi}{\alpha_l})^{3/2}\exp[-\frac{k^2}{4\alpha_l}](\frac{1}{2\alpha_l} - \frac{k_Z^2}{4\alpha_l^2}) \tag{B.6}$$

Now, we define $S_l^A(\mathbf{r})$, $P_l^A(\mathbf{r})$, and $D_l^A(\mathbf{r})$ as the followings:

$$\begin{aligned} S_l^A(\mathbf{r}) &= \frac{1}{(2\pi)^3}\int \hat{f}(k/2k_F(\mathbf{r}))\ \chi_l^{A,S}(\mathbf{k})e^{-i\mathbf{k}\cdot\mathbf{r}_A}d\mathbf{k} \\ &= \frac{(\frac{\pi}{\alpha_l})^{3/2}}{(2\pi)^2}\int_0^\infty \hat{f}(k/2k_F(\mathbf{r}))\ \exp[-\frac{k^2}{4\alpha_l}]\ J^S(k;r_A)k^2dk \end{aligned} \tag{B.7}$$

$$\begin{aligned} P_l^A(\mathbf{r}) &= \frac{1}{(2\pi)^3}\int \hat{f}(k/2k_F(\mathbf{r}))\ \chi_l^{A,P_Z}(\mathbf{k})e^{-i\mathbf{k}\cdot\mathbf{r}_A}d\mathbf{k} \\ &= \frac{(\frac{\pi}{\alpha_l})^{3/2}}{(2\pi)^2\alpha_l}\int_0^\infty \hat{f}(k/2k_F(\mathbf{r}))\ \exp[-\frac{k^2}{4\alpha_l}]\ J^P(k;r_A)k^2dk \end{aligned} \tag{B.8}$$

$$
\begin{aligned}
D_l^A(\mathbf{r}) &= \frac{1}{(2\pi)^3}\int \hat{f}(k/2k_F(\mathbf{r}))\ \chi_l^{A,D_{ZZ}}(\mathbf{k})e^{-i\mathbf{k}\cdot\mathbf{r}_A}d\mathbf{k} \\
&= \frac{1}{2\alpha_l}S_l^A - \frac{(\frac{\pi}{\alpha_l})^{3/2}}{(2\pi)^2\alpha_l^2}\int_0^\infty \hat{f}(k/2k_F(\mathbf{r})) \\
&\qquad \times \exp[-\frac{k^2}{4\alpha_l}]\ J^D(k;r_A)k^2dk
\end{aligned} \tag{B.9}
$$

Here, $J^S(k;r_A) \equiv \frac{2\sin(kr_A)}{kr_A}$, $J^P(k;r_A) \equiv \cos(\theta)\ (\frac{\sin(kr_A)}{kr_A^2} - \frac{\cos(kr_A)}{r_A})$, and

$J^D(k;r_A) \equiv \frac{kr_A\cos(kr_A)(1+3\cos(2\theta))+2\sin(kr_A)((-2+k^2r_A^2)\cos^2(\theta)+\sin^2(\theta))}{4kr_A^3}$, where θ is the azimuthal angle with respect to the molecular axis.

The nonlocal term can then be written as

$$
\begin{aligned}
V_{nl}(\mathbf{r}) = h(\mathbf{r})\{&(\textstyle\sum_l c_l^{A,S}S_l^A(\mathbf{r}) + \sum_l c_l^{A,P}P_l^A(\mathbf{r}) + \sum_l c_l^{A,D}D_l^A(\mathbf{r})) \\
&+(\textstyle\sum_m c_m^{B,S}S_m^B(\mathbf{r}) + \sum_m c_m^{B,P}P_m^B(\mathbf{r}) + \sum_m c_m^{B,D}D_m^B(\mathbf{r}))\}
\end{aligned} \tag{B.10}
$$

After substituting these defined functions, finally it gives

$$
\begin{aligned}
V_{nl}^A(\mathbf{r}) = \tfrac{h(\mathbf{r})}{(2\pi)^2}\textstyle\int_0^\infty \hat{f}(k/2k_F(\mathbf{r}))\ \{&H^{A,S}(k)\ J^S(k;r_A) + H^{A,P}(k)\ J^P(k;r_A) \\
&+H_1^{A,D}(k)\ J^S(k;r_A) + H_2^{A,D}(k)\ J^D(k;r_A)\}k^2dk
\end{aligned} \tag{B.11}
$$

$$
\begin{aligned}
V_{nl}^B(\mathbf{r}) = \tfrac{h(\mathbf{r})}{(2\pi)^2}\textstyle\int_0^\infty \hat{f}(k/2k_F(\mathbf{r}))\ \{&H^{B,S}(k)\ J^S(k;r_B) + H^{B,P}(k)\ J^P(k;r_B) \\
&+H_1^{B,D}(k)\ J^S(k;r_B) + H_2^{B,D}(k)\ J^D(k;r_B)\}k^2dk
\end{aligned} \tag{B.12}
$$

$$
V_{nl}(\mathbf{r}) = V_{nl}^A(\mathbf{r}) + V_{nl}^B(\mathbf{r}) \tag{B.13}
$$

where

$$H^{A,S}(k) = \sum_l c_l^{A,S} (\frac{\pi}{\alpha_l})^{3/2} \exp[-\frac{k^2}{4\alpha_l}] \tag{B.14}$$

$$H^{A,P}(k) = \sum_l c_l^{A,P} \frac{1}{\alpha_l} (\frac{\pi}{\alpha_l})^{3/2} \exp[-\frac{k^2}{4\alpha_l}] \tag{B.15}$$

$$H_1^{A,D}(k) = \sum_l c_l^{A,D} \frac{1}{2\alpha_l} (\frac{\pi}{\alpha_l})^{3/2} \exp[-\frac{k^2}{4\alpha_l}] \tag{B.16}$$

$$H_2^{A,D}(k) = \sum_l c_l^{A,D} \frac{1}{\alpha_l^2} (\frac{\pi}{\alpha_l})^{3/2} \exp[-\frac{k^2}{4\alpha_l}] \tag{B.17}$$

In this scheme, the k_θ integrals are evaluated analytically for each type of Gaussians. Hence, it is numerically more reliable than evaluating them numerically. Furthermore, the computational cost for this scheme is $O(N_r N_\theta N_k)$, not $O(N_r N_\theta N_k N_{k_\theta})$ if evaluated numerically. Since Eq. (B.1) is quite general in LR-based OF-DFT, this scheme is also suitable for efficient and accurate computation in diatomic molecules for other KEDFs.

Appendix C

Glossary-List of Abbreviations

1. **AILPS:** *Ab Initio* Local Pseudopotential
2. **AIMD:** *Ab Initio* Molecular Dynamics
3. **CAT:** Chacón-Alvarellos-Tarazona
4. **CC:** Coupled Cluster
5. **CI:** Configuration Interaction
6. **DFT:** Density Functional Theory
7. **FFT:** Fast Fourier Transform
8. **FWV:** Fermi Wavevector
9. **GAC:** García-González-Alvarellos-Chacón
10. **GK:** Gordon-Kim
11. **HF:** Hartree-Fock
12. **HK:** Hohenberg-Kohn
13. **KEDF:** Kinetic Energy Density Functional
14. **KP:** Kinetic Potential

15. **KS:** Kohn-Sham

16. **LDA:** Local Density Approximation

17. **LR:** Linear Response

18. **LSDA:** Local Spin Density Approximation

19. **MTF:** Modified Thomas-Fermi

20. **OF:** Orbital-Free

21. **OF-DFT:** Orbital-Free Density Functional Theory

22. **SM:** Smargiassi-Madden

23. **TBFWV:** Two-Body Fermi Wave Vector

24. **TF:** Thomas-Fermi

25. **W:** von Weizs*ä*cker

26. **WGC:** Wang-Govind-Carter

27. **WT:** Wang-Teter

BIBLIOGRAPHY

[1] R. G. Parr and W. Yang, *Density-Functional Theory of Atoms and Molecules*, (Oxford University Press, 1989).

[2] R. M. Dreizler and E. K. U. Gross, *Density Functional Theory: An Approach to the Quantum Many Body Problem*, (Springer-Verlag, Berlin, 1990).

[3] P. Hohenberg and W. Kohn, Phys. Rev. **136**, B864 (1964).

[4] W. Kohn and L. J. Sham, Phys. Rev. **140**, A1133 (1965).

[5] L. J. Sham and W. Kohn, Phys. Rev. **145**, 561 (1966).

[6] R. A. King and N. C. Handy, Phys. Chem. Chem. Phys. **2**, 5049 (2000); R. A. King and N. C. Handy, Mol. Phys. **99**, 1005 (2001).

[7] R. Car and M. Parrinello, Phys. Rev. Lett. **55**, 2471 (1985).

[8] G. Kresse and J. Hafner, Phys. Rev. B **49**, 14251 (1994).

[9] J.-D. Chai, D. Stroud, J. Hafner, and G. Kresse, Phys. Rev. B **67**, 104205 (2003).

[10] J.-D. Chai and D. Stroud, cond-mat/0408005 (2004).

[11] M. M. G. Alemany, L. J. Gallego, and D. J. González, Phys. Rev. B **70**, 134206 (2004).

[12] W. Yang, Phys. Rev. Lett. **66**, 1438 (1991); W. Kohn, Chem. Phys. Lett. **208**, 167 (1993); R. Baer and M. Head-Gordon, J. Chem. Phys. **109**, 10159 (1998); S. Goedecker, Rev. Mod. Phys. **71**, 1085 (1999).

[13] J.-D. Chai and J. D. Weeks, J. Phys. Chem B **108**, 6870 (2004).

[14] Y. A. Wang, N. Govind, and E. A. Carter, Phys. Rev. B **58**, 13465 (1998).

[15] Y. A. Wang, N. Govind, and E. A. Carter, Phys. Rev. B **60**, 16350 (1999).

[16] See e.g., Y. A. Wang and E. A. Carter, in *Theoretical Methods in Condensed Phase Chemistry*, edited by S. D. Schwartz, *Progress in Theoretical Chemistry and Physics*, (Kluwer, Boston, 2000) p. 117, and references therein.

[17] B. Zhou, Y. A. Wang, and E. A. Carter, Phys. Rev. B **6**9, 125109 (2004).

[18] B. Zhou, V. L. Ligneres, and E. A. Carter, J. Chem. Phys. **122**, 044103 (2005).

[19] E. Chacón, J. E. Alvarellos, and P. Tarazona, Phys. Rev. B **32**, 7868 (1985).

[20] P. García-González, J. E. Alvarellos, and E. Chacón, Phys. Rev. A **54**, 1897 (1996).

[21] P. García-González, J. E. Alvarellos, and E. Chacón, Phys. Rev. A **57**, 4857 (1998).

[22] M. Pearson, E. Smargiassi, and P. A. Madden, J. Physics: Condens. Matter **5**, 3221 (1993); E. Smargiassi and P. A. Madden, Phys. Rev. B **49**, 5220 (1994); M. Foley and P. A. Madden, Phys. Rev. B **53**, 10589 (1996).

[23] F. Perrot, J. Phys.: Condens. Matter **6**, 431 (1994).

[24] J. A. Alonso and L. A. Girifalco, Phys. Rev. B **17**, 3735 (1978); M. D. Glossman, L. C. Balbás, and J. A. Alonso, Chem. Phys. **196**, 455 (1995).

[25] C. Herring, Phys. Rev. A **34**, 2614 (1986).

[26] L.-W. Wang and M. P. Teter, Phys. Rev. B **45**, 13196 (1992).

[27] N. Choly and E. Kaxiras, Solid State Commun. **121**, 281 (2002).

[28] D. J. González, L. E. González, J. M. López and M. J. Stott, Phys. Rev. B **65**, 184201 (2002).

[29] J. Blanco, D. J. González, L. E. González, J. M. López and M. J. Stott, Phys. Rev. E **67**, 041204 (2003); D. J. González, L. E. González, J. M. López and M. J. Stott, Phys. Rev. E **69**, 031205 (2004).

[30] A. Delisle, D. J. González, and M. J. Stott, cond-mat/0509742 (2005).

[31] L. H. Thomas, Proc. Cambridge Phil. Soc. **23**, 542 (1927); E. Fermi, Z. Phys. **48**, 73 (1928).

[32] E. H. Lieb, Rev. Mod. Phys. **53**, 603 (1981).

[33] E. Teller, Rev. Mod. Phys. **34**, 627 (1962).

[34] N. L. Balàzs, Phys. Rev. **156**, 42 (1967).

[35] C. F. von Weizsäcker, Z. Physik **96**, 431 (1935).

[36] G. K.-L. Chan, A. J. Cohen, and N. C. Handy, J. Chem. Phys. **114**, 631 (2001).

[37] N. C. Handy, M. T. Marron, and H. J. Silverstone, Phys Rev. **180**, 45 (1969).

[38] See e.g., R. Evans, in *Fundamentals of Inhomogeneous Fluids*, edited by D. Henderson (Dekker, New York, 1992), p. 85.

[39] A. Holas and N. H. March, Phys. Rev. A **66**, 066501 (2002); I. Lindgren and S. Salomonson, Phys. Rev. A **67**, 56501 (2003).

[40] J. D. Weeks, Annu. Rev. Phys. Chem. **53**, 533 (2002).

[41] K. Katsov and J. D. Weeks, Phys. Rev. Lett. **86**, 440 (2001); K. Katsov and J. D. Weeks, J. Phys. Chem. B **105**, 6738 (2001).

[42] K. Katsov and J. D. Weeks, J. Phys. Chem. B **106**, 8429 (2002).

[43] D. R. Hamann, M. Schlüter, and C. Chiang, Phys. Rev. Lett. **43**, 1494 (1979); G. B. Bachelet, D. R. Hamann, and M. Schlüter, Phys. Rev. B **26**, 4199 (1982); D. R. Hamann, Phys. Rev. B **40**, 2980 (1989).

[44] D. Vanderbilt, Phys. Rev. B **32**, 8412 (1985).

[45] N. Troullier and J. L. Martins, Phys. Rev. B **43**, 1993 (1991).

[46] Y. Wang and R. G. Parr, Phys. Rev. A **47**, R1591 (1993).

[47] B. Wang and M. J. Stott, Phys. Rev. B **68**, 195102 (2003).

[48] L. R. Pratt, G. G. Hoffman, and R. A. Harris, J. Chem. Phys. **88**, 1818 (1988); L. R. Pratt, G. G. Hoffman, and R. A. Harris, J. Chem. Phys. **92**, 6687 (1990); G. G. Hoffman and L. R. Pratt, Mol. Phys. **82**, 245 (1994).

[49] Y.-G. Chen and J. D. Weeks, J. Chem. Phys. **118**, 7944 (2003).

[50] J. P. Perdew and S. Kurth, in *Density Functionals: Theory and Applications*, edited by D. Joubert, *Lecture Notes in Physics*, (Springer-Verlag, Berlin, 1998) p. 8, and references therein.

[51] L. J. Sham, Phys Rev. A **1**, 969 (1970).

[52] M. Levy and J. P. Perdew, Phys. Rev. A **32**, 2010 (1985).

[53] F. W. Averill and G. S. Painter, Phys. Rev. B **24**, 6795 (1981).

[54] T. D. Lee and C. N. Yang, Phys. Rev. **117**, 22 (1960); C. de Dominicis, J. Math. Phys. **3**, 983 (1962); C. de Dominicis and P.C. Martin, *ibid.* **5**, 14, 31, (1964); A. K. Rajagopal, Adv. Chem. Phys. **41**, 59 (1980); R. F. Nalewajski and R. G. Parr, J. Chem. Phys. **77**, 399 (1982).

[55] W. Yang, Phys Rev. A **34**, 4575 (1986).

[56] D. A. Kirzhnits, Sov. Phys.–JETP **5**, 64 (1957).

[57] D. A. Kirzhnits, in *Field Theoretical Methods in Many-Body Systems,* (Pergamon, London, 1967).

[58] C. H. Hodges, Can. J. Phys. 51, 1428 (1973).

[59] D. R. Murphy, Phys. Rev. A **24**, 1682 (1981).

[60] J. Lindhard, K. Dan. Vidensk. Selsk. Mat. Fys. Medd. **28**, 8 (1954).

[61] W. Jones and W. H. Young, J. Phys. C **4**, 1322 (1971).

[62] Y. Tomishima and K. Yonei, J. Phys. Soc. Jpn. **21**, 142 (1966).

[63] P. K. Acharya, L. J. Bartolotti, S. B. Sears, and R. G. Parr, Proc. Natl. Acad. Sci. USA **77**, 6978 (1980).

[64] J. L. Gázquez and J. Robles, J. Chem. Phys. **76**, 1467 (1982).

[65] L. J. Bartolotti and P. K. Acharya, J. Chem. Phys. **77**, 4576 (1982).

[66] P. K. Acharya, J. Chem. Phys. **78**, 2101 (1983).

[67] T. Kato, Commun. Pure Appl. Math. **10**, 151 (1957).

[68] P. A. M. Dirac, Proc. Cambridge Phil. Soc. **26**, 376 (1930).

[69] D. M. Ceperley, Phys. Rev. B **18**, 3126 (1978); D. M. Ceperley and B. J. Alder, Phys. Rev. Lett. **45** , 566 (1980).

[70] J. P. Perdew and A. Zunger, Phys. Rev. B **23**, 5048 (1981).

[71] A. M. Abrahams and S. L. Shapiro, Phys. Rev. A **42**, 2530 (1990).

[72] P. García-González, J. E. Alvarellos, and E. Chacón, Phys. Rev. A **54**, 1897 (1996).

[73] J. P. Perdew and Y. Wang, Phys. Rev. B **45**, 13244 (1992).

[74] A. D. Becke, Phys. Rev. A **33**, 2786 (1986).

[75] E. Clementi and E. Roetti, Atomic Data and Nuclear Data Tables **14**, 177 (1974).

[76] J. Cioslowski, Phys. Rev. A **39**, 378 (1989).

[77] I. Porras and F. J. Gálvez, Phys. Rev. A **46**, 105 (1992).

[78] R. G. Gordon and Y. S. Kim, J. Chem. Phys. **56**, 3122 (1972).

[79] A. D. Becke, J. Chem. Phys. **88**, 2547 (1988).

[80] J. M. Pérez-Jordá, A. D. Becke, and E. San-Fabián, J. Chem. Phys. **100**, 6520 (1994).

[81] D. M. Bylander and L. Kleinman, Phys. Rev. B **55**, 9432 (1997).

[82] N. H. March, Phys. Lett. A **113**, 476 (1986).

[83] A. Holas and N. H. March, Phys. Rev. A **44**, 5521 (1991).

[84] J. E. Jaffe and A. C. Hess, J. Chem Phys. **105**, 10983 (1996).

[85] S. Dhar, A. Ziegler, D. G. Kanhere, and J. Callaway, J. Chem. Phys. **82**, 868 (1985).

[86] K. P. Huber, in *American Institute of Physics Handbook*, edited by D.E. Gray (McGraw-Hill, New York, 1972).

[87] E. J. Baerends and P. Ros, Int. J. Quantum Chem. Symp. **12**, 169 (1978).

[88] L. Goodwin, R. J. Needs, and V. Heine, J. Phys.: Condes. Matter **2**, 351 (1990).